



Brains for All the Ages: Structural Neurodevelopment in Infants and Children from a Life-Span Perspective

John E. Richards¹, Wanze Xie

Department of Psychology, Institute for Mind and Brain, University of South Carolina, Columbia, SC, USA

¹Corresponding author: e-mail address: richards-john@sc.edu

Contents

1. Structural Neurodevelopment and Behavior	2
2. Neurodevelopmental MRI Database	5
2.1 The Need for Pediatric MRI Templates	5
2.2 Average MRI Templates from 2 Weeks to 89 Years	9
2.3 Priors for MRI Tissue Segmentation	15
2.4 A Common Neurodevelopmental Stereotaxic Atlas	18
2.5 Access to the Neurodevelopmental MRI Database	21
3. Applications to MRI	22
3.1 Volumetric Analysis of Brain Structural Development	22
3.2 "Study-Specific" MRI Templates and Neurostructural Development in Chinese Children	28
3.3 Nonmyelinated Axon Tissue Segmentation in Infants	33
3.4 Contribution to Methods for Studying Brain Activity	37
4. Relation to Brain–Behavior Development	42
Acknowledgments	43
References	44

Abstract

Magnetic resonance imaging (MRI) is a noninvasive method to measure brain structure and function that may be applied to human participants of all ages. This chapter reviews our recent work creating a life-span Neurodevelopmental MRI Database. It provides age-specific reference data in fine-grained age intervals from 2 weeks through 89 years. The reference data include average MRI templates, segmented tissue priors, and a common stereotaxic atlas for pediatric and adult participants. The database will be useful for neuroimaging research over a wide range of ages and may be used to make life-span comparisons. The chapter reviews the application of this database to the study of neurostructural development, including a new volumetric study of segmented brain

tissue over the life span. We also show how this database could be used to create “study-specific” MRI templates for special groups and apply this to the MRIs of Chinese children. Finally, we review recent use of the database in the study of brain activity in pediatric populations.



1. STRUCTURAL NEURODEVELOPMENT AND BEHAVIOR

Brain development occurs over the life span. We know a lot about the changes in the structure of the brain, including global structural changes (size and shape), neural changes (synaptogenesis, myelination, and tract development), and genetic and epigenetic influences on brain development. The last two decades have seen the emergence of research that shows parallels and causal relations between brain structural development and psychological-behavioral development in participants across the life span. Of special interest in this regard is the emergence of studies that have examined brain functional activity with magnetic resonance imaging (MRI) neuroimaging in its relation to cognitive or emotional development (e.g., [Braver et al., 1997](#); [Casey et al., 1995, 1998, 1997](#)). In more recent years, direct evidence for the effects of brain structural development has been shown on both cognitive development ([Rice, Viscomi, Riggins, & Redcay, 2014](#)) and emotional self-regulation ([Fjell et al., 2012](#)). This is an exciting time for those interested in brain-behavior relations across development.

The study of brain structural development has been hampered by the lack of tools to measure brain structure in typically developing humans. For many years, the study of brain development was limited to autopsy studies (e.g., [Conel, 1939–1967](#); [Huttenlocher, 1990, 1994](#); [Kinney, Brody, Kloman, & Gilles, 1988](#); [Kinney, Karthigasan, Borenshteyn, Flax, & Kirschner, 1994](#)), studies of nonhuman primates (e.g., comparative neurodevelopment, [Bourgeois, 1997](#)), or clinical populations (see [Richards, 2009](#), for discussion). A technique that may be used to examine the brain of individual participants at all ages is MRI. The MRI has been described in several places (e.g., [Huettel, Song, & McCarthy, 2004](#)). The head’s materials (skull, cerebrospinal fluid (CSF), brain, and muscles) have magnetic properties that differ based on their chemical composition. The MRI uses these differences to identify the type and location of materials inside the head. This allows for the identification, visualization, and quantification of skull, skin, CSF, white and gray matter (GM), myelination, vascularization, and other head properties. The study of brain development using MRIs has a fairly “recent”

history (e.g., [Giedd et al., 1999, 1996](#); [Jernigan et al., 1991](#)) but is increasingly becoming an important tool for studying brain development in pediatric populations.

There have been two limitations to the use of MRI for studying neurostructural development; one problem has been resolved and the other solution is “in progress” ([Section 2](#)). One limitation has been the lower age limit for the use of MRI; this problem has been solved. The MRI environment is noisy, often is in a hospital or clinical setting, and requires almost no head movement during the scan. The latter is especially true in “3D sequences.” The MRI sequence can be “two-dimensional” (2D) or “three-dimensional” (3D). The MRI emits a radio frequency (RF) pulse, which is an electromagnetic wave that excites protons which are aligned in the magnetic field. In a 2D scan, the RF pulse excites a narrow slice of the imaging volume (2D), and the magnetic changes are measured in a single 2D plane. In a 3D scan, the RF pulse excites the entire imaging volume and MRI encoding is used to distinguish the spatial areas. The 3D sequence has far greater resolution since the final scan represents the average of the entire sampled volume over the course of the sequence ([Brunner & Ernst, 1979](#)). However, the 3D sequences take longer time to complete. Any movement of the head relative to the scanner in any part of the sequence will affect the entire scan (cf., 2D sequences are shorter, and movement only affects the slice during which movement occurs). Typically, clinical pediatric participants who cannot remain still, such as infants and children, are given a mild sedation to help reduce head movements. However, this is not permitted for ethical reasons for typically developing children due to the slight risks associated with sedation. Fortunately, this problem has been solved with the use of MRI for neurostructural development. Infants and children who cannot remain still are scanned while sleeping (see [Section 2.1](#)). Children older than about 4 years are either given brief training in a mock scanner, or respond to verbal instructions. We have previously reviewed how MRIs may be done with infant participants ([Richards, 2009](#)). The problem of movement in the MRI remains a problem for functional MRI (fMRI). Young children have great difficulty with the scanner when in an alert, behaving state ([Byars et al., 2002](#)).

The second limitation to the use of MRI for studying neurostructural development has been the lack of methodological tools for conducting MRIs on “pediatric” (infants, children, and adolescents) populations. The solution to this problem is “in progress” ([Section 2](#)). Both structural and fMRI studies require standardized reference MRI volumes, including

MRI head or brain templates, tissue segmentation priors, and stereotaxic atlases (Section 2.1). Initially, this was done in Talairach space (Talairach and Tournoux, 1988; also see Talairach Atlas Database Daemon, Fox & Uecker, 2005; Lancaster, Summerlin, Rainey, Freitas, & Fox, 1997; Lancaster et al., 2000), though specific limits in the Talairach atlas (Talairach and Tournoux, 1988) limited its usefulness (Mandal, Mahajan, & Dinov, 2012). The contemporary reference system for most MRI work is based on the reference space in the “Montreal Neurological Institute” (MNI) standard (Montreal Neurological Institute brain atlas; Evans et al., 1993; Evans, Collins, & Milner, 1992; Mazziotta, Toga, Evans, Fox, & Lancaster, 1995). This reference system is based on MRIs collected from young adult participants, and their relevance for pediatric and aging populations has been questioned. The solution to this problem has been the construction of MRI reference volumes for participants across a wide range of ages and with sufficient age resolution to capture the neurostructural changes that happen during development.

This chapter reviews our work on a “Neurodevelopmental MRI Database.” The database consists of average MRI templates, tissue segmentation priors, stereotaxic atlases, and over 4000 MRI volumes of individual participants. We cover the age range from 2 weeks through 89 years of age. The database answers the problems listed above by providing MRI reference volumes for participants over a wide range of ages. Additionally, the existence of a large database of individual MRI volumes allows the investigation of brain structural development over the life span. The “Neurodevelopmental MRI Database” is a unique resource for the study of brain development. It will be useful for quantitative studies of brain development, measurement of brain activity with techniques such as fMRI and psychophysiology, and provide a standardized norm for brain development across the life span.

This chapter will do two things. First, we will spend time describing a database of reference MRI templates and accompanying materials. This “Neurodevelopmental MRI Database” covers the life span with common average MRI templates, tissue segmentation priors, and stereotaxic atlases. In addition to the reference materials, there are over 4000 MRI volumes from typically developing participants ranging in age from 2 weeks through 89 years of age. Second, we will show how this database may be used in the study of neurostructural development. We also will suggest some ways in which this database might be useful in the study of brain–behavior relations during development, though we will not review this latter topic extensively.



2. NEURODEVELOPMENTAL MRI DATABASE

2.1. The Need for Pediatric MRI Templates

The study of brain development in infants, children, and adolescents often uses MRI techniques to assess brain structure. However, many of the procedures used to analyze pediatric MRIs are based on reference data derived from adults. For example, MRI procedures often require that participant MRIs be combined into a single reference frame. Aligning the MRIs with linear or nonlinear registration to a standard MRI does this. Typically, pediatric brains have been normalized based on adult brain templates based on a single adult subject (Talairach & Tournoux, 1988) or the average of young adult participants (Evans et al., 1993; Mazziotta et al., 2001; see Mandal et al., 2012, for overview). The “MNI” template, known as the MNI-305, is one such young adult template (Collins, Neelin, Peters, & Evans, 1994; Evans, Brown, Kelly, & Peters, 1994; Joshi, Davis, Jomier, & Gerig, 2004). It was constructed with an iterative linear averaging technique based on 305 adult participants and is the *de facto* standard for defining the spatial orientation of the brain in MRI volumes. A more recent template is the “International Consortium for Brain Mapping” (ICBM) “ICBM-152.” This average MRI template was derived from 152 high-resolution 3D MRIs that were registered to the MNI-305 template (Mazziotta et al., 2001). The ICBM-152 template is distributed as the MNI-152 T1W volume with neuroimaging processing programs (e.g., FSL, Smith et al., 2004; SPM, Penny, Friston, Ashburner, Keibel, & Nichols, 2007). Such reference data include average MRI templates used for combining MRIs across participants, average-segmented GM and white matter (WM) MRI volumes used for analyzing the brain tissues, and stereotaxic atlases used to identify anatomical features in the brain.

The use of adult reference MRIs to analyze pediatric MRIs is problematic. Studies have shown problems with aligning child brains to adult brains due to more variable contours of the cortex (Hoeksma, Kenemans, Kemner, & van Engeland, 2005; Muzik, Chugani, Juhasz, Shen, & Chugani, 2000), misclassification of brain tissue (Wilke, Schmithorst, & Holland, 2002), and local and global neurostructural changes (Gogtay et al., 2004; Lenroot & Giedd, 2006; Sowell, Thompson, & Toga, 2004). In addition to differences between adult brains and pediatric brains at a given age, differential brain growth during specific developmental periods (e.g., infant infancy and child childhood) creates large variability across ages both within and between children for brain size and shape, and brain tissue

classes (Joshi et al., 2004; Muzik et al., 2000; Prastawa, Gilmore, Lin, & Gerig, 2005; Wilke et al., 2002). These and other issues have led several to conclude that the use of adult reference MRIs is inappropriate for application to pediatric MRIs and for studying brain growth and development.

A solution to this problem has been the creation of reference MRI data based on pediatric populations. For example, Altaye, Holland, Wilke, and Gaser (2008) created an infant MRI template from MRI scans that were obtained from infants from birth through 12 months of age. They reported that the use of adult templates in normalization and segmentation of infant MRIs resulted in misclassifications of tissue types and that these misclassifications were reduced when using the infant template. Similarly, we have created MRI templates based on infant participants (Sanchez, Richards, & Almlí, 2011) and a series of stereotaxic atlases in 1.5-month increments from 3 to 12 months of age (Fillmore, Richards, Phillips-Meek, Cryer, & Stevens, 2014; Phillips, Richards, Stevens, & Conington, 2013). We showed that the fit of an average template atlas to manually segmented regions was better when the age of the average template's participants matched the age of the infant. The fit of the template atlas to the manually segmented regions grew increasingly worse as the difference between the infant's and template's participants' age increased.

The problem of using reference data from young adults is not limited to infants. Although some studies have reported that children as young as 7 years of age can be adequately normalized with adult templates (Burgund et al., 2002; Kang, Burgund, Lugar, Petersen, & Schlaggar, 2003) or that the MNI-305 reference was suitable for use with spatial normalization for children at least 6 years of age (Muzik et al., 2000), the use of templates based on young adults for use with children and adolescents has been questioned. Structural variation in the brain across ages could result in spurious age differences based on an increasing disparity between the age of the participants upon which the template was based and the age of the participants in the study. Yoon, Fonov, Perusse, and Evans (2009) analyzed the brain tissue (GM and WM) distribution of young children (~8 years). They found that using an age-specific template based on 8-year-old children for normalization resulted in a considerably different tissue distribution than using a template based on adult participants. These issues may also apply to using young adult MRI templates with aging populations. There are significant changes in brain volume (Fotenos, Snyder, Girton, Morris, & Buckner, 2005), GM and WM (Ge et al., 2002; Good et al., 2001; Sato, Taki, Fukuda, & Kawashima, 2003; Sullivan, Rosenbloom, Serventi, & Pfefferbaum, 2004;

Taki et al., 2004), and overall structure during adulthood. Lemaître et al. (2005) found that beginning at age 20 there was a constant linear decline in percent of GM through the life span to late adulthood. Similar to the studies with children as participants, studies report that using an MRI template based on older adults have better results for elderly participants than using an MRI template based on young adults. For example, Huang et al. (2010) compared a study-specific template based on the older adults in their study with a template developed from young adult images for spatial normalization within an fMRI data analysis. Huang et al. (2010) found that more voxels were identified as functionally significant in older adults when the study-specific template was used. Studies comparing a study-specific template to the MNI template for volumetric brain analysis have demonstrated that using a study-specific template reduced anatomical biases in the analysis (Ashburner & Friston, 2000; Good et al., 2001; Thompson et al., 2001).

The last 10 years has seen a proliferation of MRIs of typically developing infants and children that would be useful for the construction of age-appropriate pediatric reference MRIs. A notable contribution in this regard is the NIH MRI Study of normal brain development (NIHPD). This was a multicenter study that acquired MRIs from over 400 healthy, typically developing participants 4.3–18 years of age, and participants from 2 weeks to 4 years of age (Almli, Rivkin, & McKinstry, 2007; Brain Development Cooperative Group, 2006, 2012; Lange, Froimowitz, Bigler, Lainhart, & Brain Development Cooperative Group, 2010; Leppert et al., 2009; Waber et al., 2007). This resulted in a large database of pediatric brain images, which were made widely available by the NIHPD project.

A second notable contribution to the study of structural neurodevelopment has been the development of procedures that allow the scanning of typically developing young infants. The standards and procedures for this were set by the NIHPD (Almli et al., 2007; Evans, 2005; NIH, 1998). Participants are scanned without sedation, with infants and very young children being scanned during sleep, and children older than about age 4 being scanned while awake. We use this approach in our work on the development of infant attention (Richards, 2009). Infant participants who take part in psychophysiological studies of infant attention (Richards, 2012, 2013a; Zieber & Richards, 2013) also have MRI scanning. The infant and parent come to the MRI center in the evening at the infant's typical bedtime. When the infant is asleep, it is placed on the MRI table, earplugs and headphones are put on, and then the MRI recording is done. Figure 1 shows an infant lying on the MRI bed—the headphones and cloths surrounding the



Figure 1 An infant lying on the MRI bed going into the MRI tube. The infant is covered with a sheet and has a restraining strap lightly placed across his/her body. The headphones and cloths surrounding the infant can be seen in this picture. A research assistant (left side of picture) and the parent (right side of picture) are close to the baby during the scan. The right figure shows a 5-year-old child in the same scanner. *Left figure adapted from Richards (2009).*

infant can be seen. We do this recording in awake children from 4 years of age through young adulthood (Figure 1). We often use a mock scanner room for the younger children to have the child practice good scanner behavior before the actual MRI scan. Several labs are doing routine MRI recording of individual participants and then testing the participants in behavioral/psychological experiments (Akiyama et al., 2013; Lloyd-Fox, Wu, Richards, Elwell, & Johnson, 2013). Thus, scans for infant participants from the NIHPD study and from other sources have led to a large number of MRI scans for infants (birth through 1 year), and scans for child participants from the NIHPD study and other sources have led to a large number of MRI scans for children and adolescents.

The availability of MRIs from typically developing infants, children, and adolescents has led to a proliferation of MRI reference data based on pediatric populations. Average MRI reference data have been constructed for infants (Akiyama et al., 2013; Altaye et al., 2008; Sanchez et al., 2011; Shi et al., 2010, 2011), children and adolescents (Fonov et al., 2011; Sanchez, Richards, & Almlí, 2012; Wilke et al., 2008, 2002), and adults (Fillmore, Richards, et al., 2014; Phillips et al., 2013). Some of these reference data were based on a specific age or limited ages (infants: Akiyama et al., 2013; Altaye et al., 2008; Shi et al., 2010, 2011; 8-year-olds: Yoon et al., 2009). Average MRI templates have been constructed with the wider age ranges of the NIHPD database. These include: (1) Wilke, Holland, Altaye, and Caser (2008) created a template-building platform (Template-O-Matic) through which researchers could specify the age range and sex of the resulting templates, which were based on linear registration techniques and (2) Fonov

et al. (2011) constructed age-appropriate atlases that provided templates with significant anatomical detail for six age ranges with a width of 4–6 years each that were grouped according to estimated pubertal status: 4.5–8.5 years, pre-puberty; 7.0–11.0 years, pre- to early puberty; 7.5–13.5 years, pre- to mid-puberty; 10.0–14.0 years, early-to-advanced puberty; and 13.0–18.5 years, mid- to postpuberty. [Section 2.2](#) describes a life-span Neurodevelopmental MRI Database that we have constructed.

2.2. Average MRI Templates from 2 Weeks to 89 Years

Our contribution to this work has been the acquisition of MRI volumes from typically developing participant across the life span and construction of age-specific templates; we call this the “Neurodevelopmental MRI Database.” The MRI volumes consist of MRIs collected from over 4000 participants who ranged in age from 2 weeks through 89 years at the time of the scan. These data consist at least of whole-head T1-weighted MRI scans. Several participants also had other scans (e.g., T2-weighted MRI scans), diffusion tensor imaging (DTI, for axon pathways), and MRI spectroscopy scans (for relative concentrations of brain metabolites), though we have included only the T1W and T2W scans in the database. Each MRI scan is processed in a pipeline to do brain extraction (“skull-stripping”; [Smith et al., 2004](#); [Woolrich et al., 2009](#)), tissue segmentation (GM, WM, and other materials), skull and scalp identification, and linear and nonlinear registration to a number of MRI reference templates. The MRI volumes came from several sources: (1) locally collected data from the McCausland Center for Brain Imaging (MCBI; <http://www.mccauslandcenter.sc.edu>) with ages from 3 months through about 34 years; all are 3T strength, 3D scans, with both T1W and T2W sequences; (2) NIHDP Objective 2 data ([Almli et al., 2007](#); http://www.bic.mni.mcgill.ca/nihpd/info/data_access.html), with ages from 2 weeks through 4.4 years; all are 1.5T strength, 2D scans, with both T1W and T2W sequences; (3) NIHDP Objective 1 data ([Waber et al., 2007](#)) with ages from 4.5 years through about 18 years; all are 1.5T strength, with both T1W and T2W scans, most of the scans from 4.5 through 6 years are 2D sequences, and the older scans are 3D sequences; (4) Autism Brain Imaging Data Exchange (ABIDE; [Di Martino et al., 2013](#); http://fcon_1000.projects.nitrc.org/indi/abide/); 3T strength, 3D scans, T1W sequences; (5) Information Extracted from Medical Images database (IXI; [Ericsson, Alijabar, & Rueckert, 2008](#); [Heckemann et al., 2003](#); <http://biomedic.doc.ic.ac.uk/brain-development/>

[index.php?n=Main.Datasets](#)); with scans from both 3T and 1.5T scanners, 3D sequences, T1W and T2W sequences; and (6) Open Access Series of Imaging Studies (OASIS; Marcus, Fotenos, Csernansky, Morris, & Buckner, 2010; Marcus et al., 2007; <http://www.oasis-brains.org>); with 1.5T strength scans, 3D sequences, T1W sequences. We also have obtained a number of scans from other sites, which are used in collaborative studies (e.g., Center for Brain and Cognitive Development, Lloyd-Fox et al., 2014).

A subset of the MRI volumes has been used in studies to create reference MRI data for a wide range of ages. (1) Sanchez et al. (2011) used MCBI and NIHPD Objective 2 data to create infant and preschool average MRI templates. These were done in 1.5-month intervals in the first 9 month, 3-month intervals from 9 to 18 months, then at 2, 2.5, 3, and 4.0 years. (2) Sanchez et al. (2012) used MCBI and NIHPD Objective 1 data to create average MRI templates from 4.5 through young adulthood. These templates exist for age groups of 6-months (e.g., 4.5, 5.0, and 5.5 years) through 19.5 years of age, and a single “young adult” template generated from participants from 20 to 24 years of age. The 20- to 24-year-old average was constructed to create an adult comparison template similar to the ages of the MNI and ICBM templates (Collins et al., 1994; Evans et al., 1994, 1993; Joshi et al., 2004; Mazziotta et al., 2001). (3) Phillips et al. (2013; also see Fillmore, Richards, et al., 2014) created adult templates in 5-year increments from 20 years of age through 89 years of age (e.g., 20–24 years, 30–34 years, through 85–89 years). These templates were compiled from MCBI data (20–34 years), the NIHPD Objective 1 (about 25 in 20–24 year group), IXI data (20–89 years), and OASIS data (20–89 years).

The details for the construction of the average MRI templates are found in the original articles (Fillmore, Richards, et al., 2014; Phillips et al., 2013; Sanchez et al., 2011, 2012). The procedure used a tentative average volume from the MRIs of the participants of a specific age range. The initial volumes were oriented to the ICBM-152 template. Due to the initial orientation, the templates are loosely oriented to the ICBM-152 volume. The individual volumes were registered to this tentative average with nonlinear registration (ANTS, “Advanced Normalization Tools”; Avants, Epstein, Grossman, & Gee, 2008; Avants et al., 2011), and then the average was reconstructed. Nonlinear registration preserves fine details in the average MRI template when compared with linear registration techniques (Ashburner & Friston, 2000). We used an iterative averaging procedure (see Fonov et al., 2011; Guimond, Meunier, & Thirion, 2000; Yoon et al., 2009, for examples of similar iterative routine; see Mandal et al., 2012, for a discussion of MRI

template construction methods). The iterative procedure avoids biasing the templates to adult reference data. Our database is unique in providing fine-grained age intervals with sufficient numbers of participants in each age group to provide reliable averages. It provides consistent methods and format for a database of normative age-appropriate average MRI templates across the life span.

The MRI volumes in the database differ in scanning sequence details that affected the quality of some of our average templates. The MCBI sequences are from a Siemens Tim Trio 3T scanner. All T1W sequences at this site are 3D scans. This is important because the 3D sequence has far greater resolution than 2D scans, which is critical for average MRI template construction. The T2W scans are either 2D (infants) or 3D (children through adults) sequences. The NIHPD Objective 2 study used 1.5T, 2D sequences. They did this due to predicted time constraints for the entire set of sequences and to insure that they had a short duration T1-weighted scan for the youngest participants. This provides scans of inferior resolution to 3T–3D scans. Thus, when creating the database, we have created separate 1.5T averages, combined 1.5T and 3.0T scans, and separate 3.0T scans. The ABIDE data are all 3.0T, 3D scans; the OASIS and IXI have 3D scans and a mix of 1.5T and 3.0T strengths.

We selected age intervals for each average scan to provide fine-grained age-selective MRI templates while keeping sufficient numbers of participants for the average. [Table 1](#) shows the age intervals, numbers of participants for each average, and the numbers of participants for 1.5T and 3.0T scans in the average. The “Combined” templates include both 1.5T and 3.0T averages and cover the entire age range. We prefer the averages made of 3.0T participant MRIs for our own work ([Fillmore, Phillips-Meek, & Richards, 2014](#); [Phillips et al., 2013](#); [Richards, 2012, 2013b](#); [Xie, Richards, Lei, Kang, & Gong, 2014a, 2014b](#); [Zieber & Richards, 2013](#)). For infants, the 1–5T scans come from the NIHPD open source database and are 2D scans. Our MCBI 3T–3D scans of infants have higher spatial resolution and better signal-to-noise ratio than the NIHPD scans. For children (e.g., [Xie et al., 2014a, 2014b](#)), the spatial resolution of the NIHPD 1–5T scans is adequate given the size of the children head, whereas the signal resolution (signal-to-noise ratio) is better in the 3T than in the 1.5T scans. For each age, we constructed a whole-head MRI average, separately for T1-weighted and T2-weighted scans. We used the extracted brain from the whole-head MRIs from the individual participants to create a separate average MRI template for the brain, separately for T1- and T2-weighted scans.

Table 1 Age and Number of Participants for the 1.5T, 3.0T, and Combined Average MRI Templates
Pediatric Populations

<i>Infants</i>	<i>1.5T</i>	<i>3.0T</i>	<i>Combined</i>
2–0 Weeks	23		23
3–0 Months	22	14	36
4–5 Months		12	12
6–0 Months	32	14	46
7–5 Months		11	11
9–0 Months	29	10	39
12–0 Months	25	10	35
<i>Preschool</i>	<i>1.5T</i>	<i>3.0T</i>	<i>Total</i>
15–0 Months	32		32
18–0 Months	32		32
2–0 Years	27		27
2–5 Years	31		31
3–0 Years	22		22
4–0 Years	19	4	19
<i>Children</i>	<i>1.5T</i>	<i>3.0T</i>	<i>Total</i>
4–5 Years	9		9
5–0 Years	14		14
5–5 Years	17		17
6–0 Years	27	10	37
6–5 Years	36		36
7–0 Years	27		27
7–5 Years	44		44
8–0 Years	46	19	56
8–5 Years	40	12	40
9–0 Years	46		46
9–5 Years	41	10	41
10–0 Years	62	16	72
10–5 Years	52		52

Table 1 Age and Number of Participants for the 1.5T, 3.0T, and Combined Average MRI Templates—cont'd
Pediatric Populations

Adolescents	1.5T	3.0T	Total
11–0 Years	31		31
11–5 Years	40		40
12–0 Years	37	15	47
12–5 Years	30		30
13–0 Years	34	11	34
13–5 Years	29	19	29
14–0 Years	32	30	42
14–5 Years	30	1	31
15–0 Years	32		32
15–5 Years	23		23
16–0 Years	34	13	44
16–5 Years	28	1	29
17–0 Years	25		25
17–5 Years	25		25
Adults			
Adults	1.5T	3.0T	Total
18–0 Years	18	20	28
18–5 Years	12	23	29
19–0 Years	10	17	23
19–5 Years	5	21	22
20–24 Years	157	117	244
25–29 Years	86	24	101
30–34 Years	63	34	79
35–39 Years	50		50
40–44 Years	61		61
45–49 Years	65		65
50–54 Years	57		57

Continued

Table 1 Age and Number of Participants for the 1.5T, 3.0T, and Combined Average MRI Templates—cont'd
Adults

55–59 Years	73	73
60–64 Years	83	83
65–69 Years	89	89
70–74 Years	101	101
75–79 Years	61	61
80–84 Years	62	62
85–89 Years	36	36

The “Combined” column represents the total number of participants in the combined (1.5T + 3.0T) atlas, which includes all 1.5T MRIs and part or all of the 3.0T MRIs, as in the original publications (Fillmore, Richards, et al., 2014; Phillips et al., 2013; Sanchez et al., 2011, 2012). The templates based on the 3T MRIs differ from those in the original publications because we continue to add 3T MRIs to our database and update the 3T templates.

The resulting MRI templates are illustrated in Figures 2 and 3. Figure 2 shows the mid-sagittal slice of the whole-head average MRI template for selected ages. This is shown preserving the relative size of the heads across the ages. The rapid head size increase may be seen from about birth through 18 months of age, which then continues at a slower pace through adolescence. Small detailed changes may be seen in this figure in the cortical and subcortical anatomy in the shape and topological arrangement of brain features across the age range. The full set of whole-head average templates is given in the original articles (Fillmore, Richards, et al., 2014; Phillips et al., 2013; Sanchez et al., 2011, 2012).

Figure 3 shows an axial slice of the brain average MRI template for selected ages at the level of the anterior commissure. The averages are shown as the same size irrespective of actual template size. The average templates show regional patterns of myelination in the first 2 years. The posterior limb of the internal capsule is fully myelinated at 3 months; posterior regions of the hemispheres (e.g., occipital and temporal lobes) show myelination at 6 months, and seemingly full coverage of myelination by about 12 or 15 months of age. We know that myelination continues throughout the period of childhood and well into adolescence (Toga, Thompson, & Sowell, 2006). At the youngest ages, the WM tracts have lower MRI voxel values and thus appear darker than GM nuclei in a T1W scan. The lower voxel values reflect the fact that unmyelinated axons have a faster

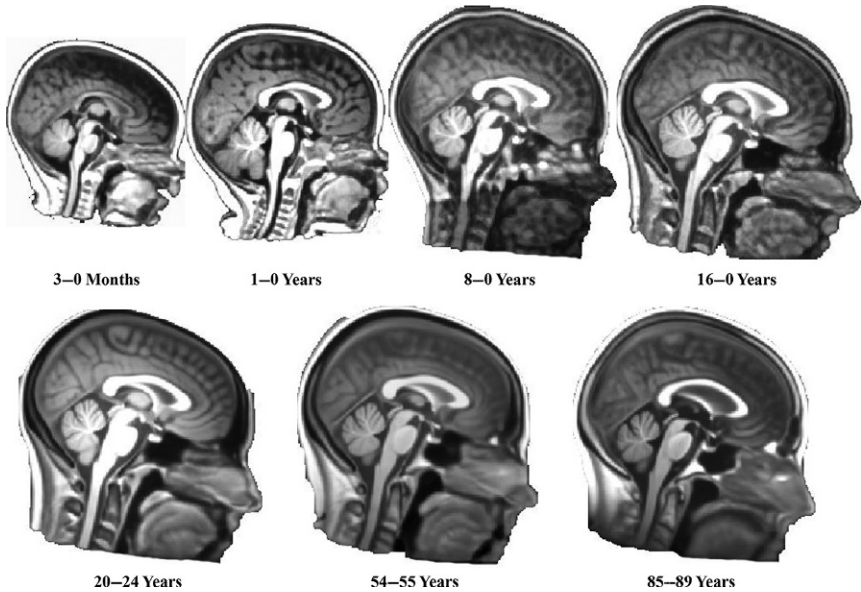


Figure 2 Whole-head average MRI templates for selected ages from the Neurodevelopmental MRI Database. This is a midsagittal slice, and heads are oriented approximately with the MNI template orientation. The size of the figures is proportional to the size of the average template for that age.

T1-relaxation time and thus have less magnetic energy than GM on the scan. Through childhood and into adulthood, the WM tracts become more intense (higher voxel values) than GM nuclei, since the T1-relaxation time of myelin is longer than that of GM. The relative thickness of the GM appears to decline from the youngest templates through about young adulthood (20–24-year-old template) with a corresponding increase in the amount of WM. Gradual brain atrophy becomes noticeable at the oldest ages. Despite the wide variety of ages, sources of the MRI data collection, and varieties in scanning sequence, the average MRI templates are consistent for level of detail and clarity. These developmental changes in the brain are consistent with previously established patterns of brain development and provide quantitative assessment tools for this analysis (see [Section 3](#)).

2.3. Priors for MRI Tissue Segmentation

A common task in brain structural analysis is to determine the location and quantity of “GM” and “WM”. GM consists of neuronal cell bodies and nuclei (groups of neuronal cell bodies), and WM consists of myelinated

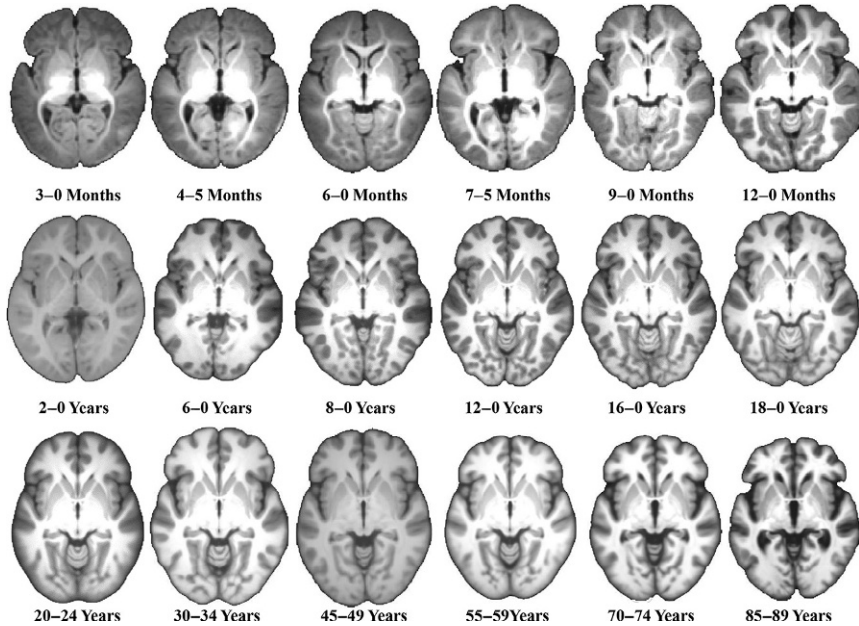


Figure 3 Brain average MRI templates for selected ages from the Neurodevelopmental MRI Database. This is an axial slice at the level of the anterior commissure. The 2–0 years template is based entirely on 1.5T MRI volumes, the mid- to late-adults are based primarily on 1.5T MRI volumes, and the rest are based on 3T volumes. The brains from different ages are shown as the same size, though they differ in size for the templates (cf., Figure 2).

axons. The evaluation of the volume and location of the GM and WM is critical in neurostructural developmental research.

Segmentation procedures use the MRI to classify brain tissue into GM, WM, and “other matter” (OM). This is often done in MRI analysis with the use of “segmented priors.” Segmented priors are patterns of GM and WM that are found in the participants who were used to construct reference MRI data. In segmenting analyses, the individual participant MRI is registered to the reference MRI template, the GM and WM segmenting priors are transformed into the participant space, and the priors are used as the first approximation of the GM and WM extent and distribution for that participant. Computer programs then use the priors and the participant MRI to segment the GM and WM tissue. Finally, tissue volume and location are then assessed for the individual participant. This analysis is done on a “T1-weighted” MRI sequence, which is designed to show maximum differentiation of GM and WM and distinguish GM/WM from other tissues in the brain (OM).

Tissue segmentation has been a major issue for neurostructural research with pediatric populations. There are major changes in the overall pattern of myelination in the first 2 years (e.g., [Figure 3](#)). This is extremely obvious in the infancy period, particularly in the first 9 months when major lobes have no myelinated axons (e.g., [Figure 3](#)). From 2 years through adolescence, there is a continuing increase in amount of myelination and changes in the structure and location of myelinated axonal pathways. The rapid growth occurring during birth through preschool years creates large variability within and between children for brain size, shape, and tissue classes ([Joshi et al., 2004](#); [Muzik et al., 2000](#); [Prastawa et al., 2005](#); [Wilke et al., 2002](#)). Misclassification of brain tissue is a commonly cited problem when using adult reference data (average MRI templates and segmented priors) in pediatric populations ([Altaye et al., 2008](#); [Yoon et al., 2009](#); [Wilke et al., 2002](#)). For example, [Yoon et al. \(2009\)](#) found that the distribution of brain tissue was different in 8-year-olds using an age-specific or an adult template. A resolution to this issue is to construct segmented priors on pediatric data.

Segmented priors were constructed for the Neurodevelopmental MRI Database. Individual participants had patterns of GM and WM identified with the “FSL FAST” computer program (FMRIB’s Automated Segmentation Tool; [Zhang, Brady, & Smith, 2001](#)). Then, the participant’s brain MRI volume was registered to its age-appropriate average MRI template, and the individuals’ GM and WM probability volumes were normalized into the reference space. Finally, average GM and WM probability volumes were then constructed. Note here that some computer programs actually create a two-class segmenting volume, and label the rest of the brain as “CSF.” However, the non-GM/non-WM tissue consists of glia, CSF, meninges, and other materials that are inside the part of the MRI extracted as the brain. We prefer to call this “OM” when creating our segmenting priors. We use the T2-weighted MRI to identify CSF in the head. T2 relaxation times in structural MRIs are substantially different in water (CSF) and matter (WM, GM, and other materials) so that voxels with large T2 values in the T2-weighted volumes come from CSF. The CSF is identified by using extracting voxels based on a threshold value for the T2-weighted volume. We calculate a separate probability volume for T2W-derived CSF. These constitute the segmented priors for our reference data.

[Figure 4](#) shows the GM- and WM-segmented priors for selected ages. The changes in the segmented priors follow the changes in myelination seen in the average MRI templates (cf. [Figures 3 and 4](#)). There are extremely vivid regional patterns of myelination in the first 12 months, substantial

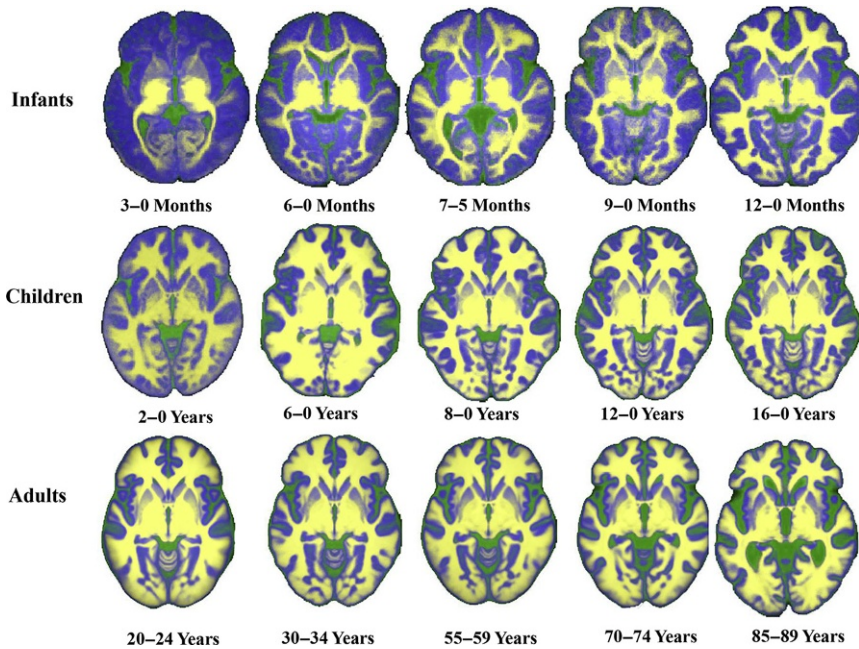


Figure 4 Tissue segmentation priors for selected ages for average MRI templates. The brightness of the colors represent the probability that a voxel belongs to the GM (blue (dark gray in the print version)), WM (yellow (white in the print version)), or “other matter” (green (gray in the print version)) category. Note the large changes in WM over the first year, due to myelination of axons over this age. The brains from the different ages are shown as the same size.

changes over the first 2 years, and gradual changes through adolescence. There are decreases in WM volume that occur in adulthood, particularly after the middle adult years (Section 3.1). These decreases are more gradual and of lesser volume than those occurring in childhood and so are not apparent in these figures.

2.4. A Common Neurodevelopmental Stereotaxic Atlas

A common stereotaxic atlas for the MRI reference data will aid the study of structural neurodevelopment. The identification of anatomical regions in MRI analysis is typically done with stereotaxic atlas MRI volumes in the same spatial system as average MRI templates. Stereotaxic atlas MRI volumes classify each voxel in the volume according to its anatomical name (e.g., macroanatomical names, cerebral lobes, axonal tracts, Brodmann numbers). For example, the ICBM152 average MRI template is accompanied by the

Harvard–Oxford Cortical atlas (Desikan et al., 2006) and the MNI structural atlas (Mazziotta et al., 2001). Other atlases are based on specific average MRI templates (e.g. LONI Probabilistic Brain Atlas, LPBA40, Shattuck et al., 2008; Hammers atlases: Hammers et al., 2003; Heckemann, Hajnal, Aljabar, Rueckert, & Hammers, 2006; Heckemann et al., 2003).

It is not surprising that stereotaxic atlases based on adult MRI reference data are unsatisfactory for pediatric populations. Similar to segmented priors, the use of stereotaxic atlas is done by registering the individual participant MRI to the reference average MRI template and then transforming the stereotaxic atlas for the reference volume into participant space. The registration (or misregistration) of the child to the reference volume may lead to spatial errors for the transformed stereotaxic atlas. The topological arrangement of the brain for a young child, particularly in the infancy period, is substantially different than the arrangement of the adult brain. The topological arrangement differs because the newborns brain is substantially smaller in volume and the skull bones are unsutured, likely so the head will be malleable when passing through the birth canal. As the brain grows and the skull bones merge, the brain expands against the skull and the brains topological arrangement relative to the skull changes. Also, there may be specific brain regions existing in adults that are may not even exist in infants! For example, axonal tracts are undefined in infants due to large areas of unmyelinated axons. Similarly, synaptogenesis, which is the primary cause of the rapid increases in GM in infancy, results in cytoarchitectural differentiation of brain regions that will be defined in adults. The lack of myelination and synaptic configuration in infants results in some brain areas existing in adults being undefined or indiscriminable in infants.

This problem has been addressed by creating stereotaxic atlases based on pediatric reference data. For example, Shi et al. (2011) combined simple automatic registration with the majority vote method. They registered the brains of ninety-five 2-year-olds to the AAL atlas (automatic anatomical labeling atlas; Tzourio-Mazoyer et al., 2002) to create a representative 2-year-old atlas. They then propagated the 2-year-old atlases down to the brains of those same participants as 1-year-olds and as newborns. Akiyama et al. (2013) created an adaption of the AAL atlas for an average MRI template based on 6-month-old infants. Gousias et al. (2008) use a method to create a stereotaxic atlas for individual 2 year-old participants based on the Hammers atlas (Hammers et al., 2003).

We have begun to address this issue by creating methods for constructing a lobar atlas, the LPBA40 atlas, and the Hammers atlas for pediatric

participants (Fillmore, Phillips-Meek, et al., 2014; Phillips et al., 2013). First, we have created a lobar atlas identifying the major cortical lobes, brainstem, cerebellum, and some subcortical and sublobar areas. This has been done on all infant reference data ages (3T average MRI volumes for 3, 4.5, 6, 7.5, 9, and 12 months), selected child/adolescent ages (8, 12, and 18 years), and for the young adults (20–24 years).

Second, we have adapted the methods of Gousias et al. (2008) that take manually segmented brains from individual participants (adults) and create an atlas for an individual participant (infants, children, adolescents, and adults) based on the adult manual segmentations. We can generate a stereotaxic atlas for each participant MRI in the Neurodevelopmental MRI Database based on the LONI Probabilistic Brain Atlas project (56 manually delineated areas; LPBA40; Shattuck et al., 2008) or the Hammers adult brain atlas (83 manually delineated areas; Hammers atlases: Hammers et al., 2003; Heckemann et al., 2006, 2003). The automatic labeling procedure compares very well to manually segmented volumes for our infant participants and infant MRI reference data (Fillmore, Phillips-Meek, et al., 2014; Phillips et al., 2013). So in addition to the participant T1W, T2W, brain, and segmented tissue volumes, we also have two segmented stereotaxic atlases for each participant in the database.

The two atlases for each individual were used to create stereotaxic atlas MRI volumes for selected average MRI volumes. Similar to the segmented prior reference volumes, the individual participants were registered to the relevant age-appropriate average MRI reference volume, and the individual participant atlas volumes were transformed to the reference volume. A procedure was then used to get the information from all individual participants to construct an MRI stereotaxic reference volume that has the probability of each voxel belonging to one of the atlas segments, i.e., tissue types, and a “majority vote” to classify each voxel into a corresponding segment. We have stereotaxic atlas MRI volumes for all the infant ages (3T average MRI volumes, for 3, 4.5, 6, 7.5, 9, and 12 months), selected child/adolescent ages (2, 3, 4, 8, 12, and 18 years), and for the young adults (20–24 years). We are in the process of applying this procedure to child and adolescent data (e.g., 4 years to 18 years in 2-year increments). We may pursue this procedure with our adult data.

Figure 5 shows some examples of the stereotaxic atlas for infants, children, and adults. The top rows show the lobar and Hammers segmenting atlases for all infant ages on the axial brain slice at the level of the anterior commissure (i.e., corresponding to Figure 3). The third row shows the

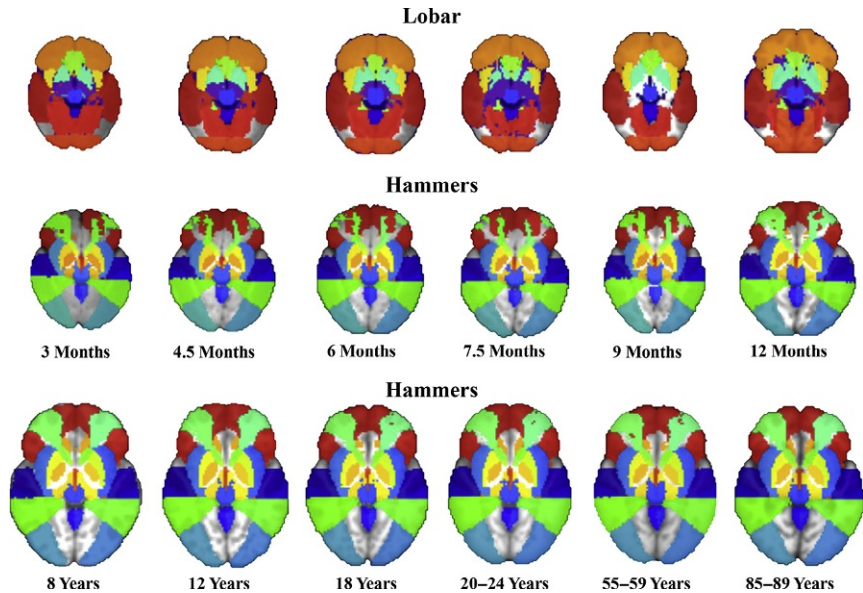


Figure 5 Stereotaxic atlas label set for the infant manual lobar atlas (first row), infant Hammers atlas (second row), and selected ages Hammers atlas (third row). A complete infant atlas set exists (lobar, Hammers, LPBA40), atlas sets exist for selected ages, and atlases for other age groups are being generated (e.g., child to adolescence from 4 to 18 years). The colors (different shades of gray in the print version) represent the label from the atlas in which a voxel is classified. Note the comparability of the segmented regions across the ages.

Hammers segmenting atlas for selected adult ages. The resulting atlases represent a common stereotaxic atlas from birth to young adulthood and should prove beneficial for neurostructural developmental work.

2.5. Access to the Neurodevelopmental MRI Database

We are very interested in encouraging the developmental neuroscience community to use the average MRI templates, segmenting priors, and atlases. These three types of data and individual participant MRI volumes represent our “Neurodevelopmental MRI Database.” The age-specific neurodevelopmental reference MRI data are available on line (<http://jerlab.psych.sc.edu/NeurodevelopmentalMRIDatabase/>). We include the average MRI templates (e.g., Figures 2 and 3), the segmenting priors for each MRI template (Figure 4), and stereotaxic atlases for selected ages (Figure 5; e.g., infants: Fillmore, Phillips-Meek, et al., 2014; Phillips et al., 2013; 20- to 24-year-old age range). These are publicly available to

researchers for clinical and experimental studies of normal and pathological brain development. Data access is limited to scientific professionals for research purposes. These data are available for instructional purposes to faculty or laboratory supervisors. We are considering putting these data on “Databrary” (databrary.org; Adolph, Gilmore, Freeman, Sanderson, & Millman, 2012), which is an open data library for development science whose goal is to provide a platform for a repository for data management, collaboration, and open sharing. We are in the process of evaluating the “Databrary” site to house these data. The individual MRI volumes are not available on the site. This is due to privacy concerns, treatment of human subjects issues, and database restrictions from our publically acquired volumes (ABIDE, IXI, NIHPD, and OASIS). We also receive MRIs from sites for collaborative work (e.g., Lloyd-Fox et al., 2013; Lloyd-Fox et al., 2014; Xie et al., 2014a, 2014b) that cannot be shared.

Figure 6 shows a screen shot of the home screen for the reference data. Interested users should contact John E. Richards (richards-john@sc.edu) for access (see Request tab), and instructions for access are included on the site (see Access tab). The template volumes are in compressed NIFTI format (<http://nifti.nimh.nih.gov/>). The data are on a file server that may be accessed with the Secure Shell (SSH) file transfer protocols (SCP or SFTP). The original, individual MR brain scans and behavioral data from the NIHPD can be obtained from their Web site (<https://nihpd.crbs.ucsd.edu/nihpd/info/index.html>). The original individual MR brain scans for the ABIDE (http://fcon_1000.projects.nitrc.org/indi/abide/), IXI (database <http://biomedic.doc.ic.ac.uk/brain-development/index.php?n=Main.Datasets>), and OASIS (<http://www.oasis-brains.org>) are available at those Web sites for public access.



3. APPLICATIONS TO MRI

3.1. Volumetric Analysis of Brain Structural Development

The MRI technique provides a noninvasive method to study human brain development. Over the past two decades, a few studies using this technique have been conducted to study neurostructural development during infancy (Fan et al., 2011; Knickmeyer et al., 2008), childhood and adolescence (e.g., Giedd et al., 1999; Lenroot et al., 2007; see review, for Sowell et al., 2004), and adulthood (e.g., Fotenos et al., 2005; Lemaître et al., 2005; Taki et al., 2004). The analysis of brain development in these studies across the life span has been from different investigations that may have used different methods, limited participants age ranges, and MRI types. An investigation showing

Neurodevelopmental MRI Database


John E. Richards, University of South Carolina

Home	Citations	Description	Ages and Templates
Cortical Sources	Access	Request	

This is a database of average MRIs and associated MRI volumes for developmental MRI work. It consists of average MRI templates, segmented partial volume estimate volumes for GM, WM, T2W-derived CSF ([Description](#)). The database is separated into head-based and brain-based averages. The data are separated by ages in months, years, 6-month, or 5-year intervals ([Ages and Templates](#)). The templates are grouped into first year (2 weeks through 12 months), early childhood (15 months through 4 years), childhood (4 years through 10 years), adolescence (10.5 years through 17.5 years) and adults (18 years through 89 years).

Tools for cortical source analysis of EEG and ERP are provided. These tools are based on the average MRI templates, segmenting, and atlases.

Terms of use: The MRI templates from this database are freely available and distributed for scientific work. These should not be distributed to others without explicit permission from JER, and should not be used in commercial applications. Publications from this work should cite the publications for the data upon which these templates are based ([Citations](#)). JER retains all copyrights to the templates.

 Neurodevelopmental MRI Database by John E. Richards is licensed under a [Creative Commons Attribution-NonCommercial-NoDerivs 3.0 Unported License](#).
Based on a work at <http://jerlab.psych.sc.edu/NeurodevelopmentalMRIDatabase/>

Contact John E. Richards (<http://jerlab.psych.sc.edu>, richards-john@sc.edu) for access to the volumes.

Created 2010-10-09

Figure 6 Screen shot of the Neurodevelopmental MRI Database Web site (<http://jerlab.psych.sc.edu/NeurodevelopmentalMRIDatabase/>).

brain development across the entire life span would add to this body of knowledge.

The first 2 years of life are the most dynamic period of human postnatal brain development. Knowledge regarding brain development in this period was limited until recent work applied MRI technique to investigate brain development in infancy. For instance, [Knickmeyer et al. \(2008\)](#) studied brain development in typically developing infants from birth to 2 years: 84 infants at 2–4 weeks, 35 at 1 year, and 26 at 2 years. They found that infant total brain volume increased by 100% during the first year and by 15% in the second year. Brain GM changed dramatically by 149% in the first year, whereas WM development was slower (11% increase). These results implied that human brain volume developed substantially in the first year of life,

driven primarily by the development of GM and cerebellum. In parallel with these brain volumetric developments, infant brain anatomical networks from different regions also developed rapidly during the first 2 years (Fan et al., 2011; Gao et al., 2009).

Researchers have used structural MRI to study brain development in childhood and adolescence since the 1990s (e.g., Giedd et al., 1999, 1996; Jernigan et al., 1991; Lenroot et al., 2007; Sowell et al., 2004). A common finding across studies has been that total brain volume increased from early childhood to adolescence, peaking at about age 10.5 years for females and 14.5 years for males. Global GM development followed an inverted U-shape peaking at about 8- (females) to 9- (males) years-old; however, different cerebral lobes showed different developmental patterns. For example, GM in frontal and parietal lobes increased to a maximum amount at roughly 10–12 years, whereas GM in temporal lobes increased through childhood and adolescence with evidence of significant decline during late adolescence (Giedd et al., 1999). In contrast, WM development followed a linear pattern from early childhood to young adults. One reason for GM decrease is the synaptic elimination or pruning. The increase of WM may indicate the development of brain networks and communication between brain structures. These changes in brain structures have been linked to behavioral changes (e.g., the development of frontal lobe is related to behavioral inhibition in adolescence; see Section 4).

Volumetric brain changes continue to occur during adulthood. Fotenos et al. (2005) measured whole-brain volume changes in participants from 18 to 97 years. They reported that whole-brain volume decline was detected by age 30, and the mean decline in total volume was constant after age 65. A common strategy is to distinguish the changes in partial volume estimates of GM, WM, and less often, CSF. The most consistent partial volume change is a reduction in GM volume. Several studies have reported GM decline in subjects beginning at age 20 with a constant linear reduction across the span of early-to-late adulthood (Ge et al., 2002; Lemaître et al., 2005; Sullivan et al., 2004; Taki et al., 2004). Changes in WM volume have been found but are not as consistent in the literature. Ge et al. (2002) reported WM changes in a quadratic pattern, with slight increases until age 40, and decreases thereafter. Salat et al. (2009) reported a quadratic relationship between WM volume and age, with relative preservation or rise in volume until the late 1950s, followed by a steep decline. An associated linear increase in CSF volume has also been reported. This finding is consistent across volumetric studies that report CSF results (Good et al., 2001; Lemaître et al., 2005; Smith, Chebrolu, Wekstein, Schmitt, & Markesbery, 2007).

We used the individual volumes from the Neurodevelopmental MRI Database to analyze volumetric changes across the life span. We first analyzed global brain and head volume development across life-span. [Figure 7](#) (left columns) shows the changes in brain, inner skull, outer skull, and head volume as a function of age from 2 weeks through 89 years. Brain and skull volume development both showed an inverted U-shape pattern peaking during adolescence with a gradual decline thereafter through adulthood. Total head volume, however, showed increasing levels through age 30 with little decline in volume during adulthood. The logarithmic scale ([Figure 7](#), lower left panel) shows a gradual increase in all four volume measures as a function of the \log_2 (age) scale. This type of growth is typical of growth scales for nearly all human physiological systems.

The GM and WM development of the participant MRIs was also measured. For this analysis, we used the segmented priors from the age-specific reference volume for each individual. We have found that using these priors resulted in the most accurate measure of partial volumes ([Fillmore, Richards, et al., 2014; Sanchez et al., 2012](#)). Our results are presented in [Figure 7](#) (right columns). The changes in GM showed increases at a very rapid rate from

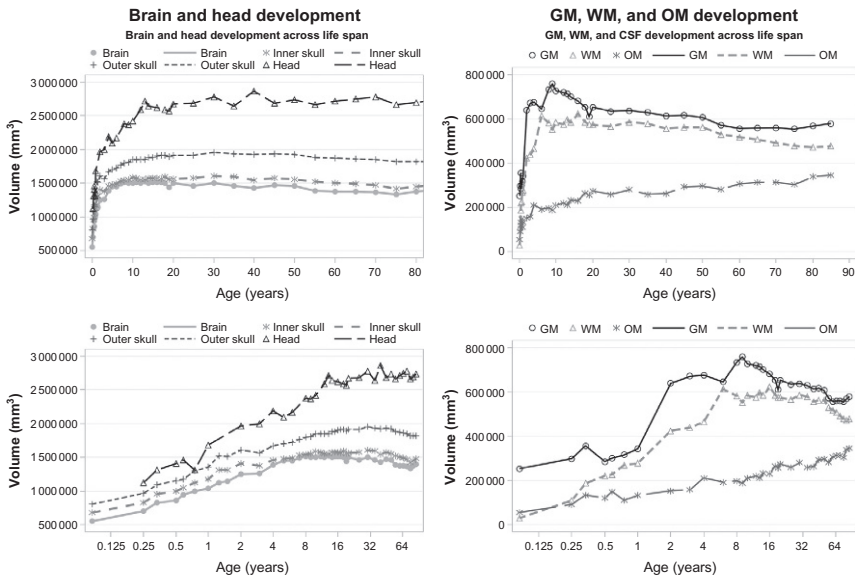


Figure 7 Neurostructural development across the life span. Changes in overall volume (head, skull, and brain) are shown on the left panels, and changes in segmented tissue volume (GM, WM, and “Other Matter”) are shown on the right panels. The top panels show volumes as a function of age, whereas the bottom panels show changes in volume as function of $\log(\text{age})$. The error bars represent the standard error of the mean (SE).

infancy through about 10–12 years, followed by a linear decline through late adulthood. Conversely, WM changes had a more gradual increase through childhood and adolescence, a plateau through most of the adult years, with declining volumes happening only after about 50 years of age. The “OM” category, which includes several types of tissue, showed a gradual increase over the entire life span. An interesting finding is that the decline in GM and WM volume during adulthood were offset by increases in OM (Figure 7, left figures). This resulted in less overall brain volume decline than would be expected from GM and WM alone (Figure 7, right figures). The increases in “OM” may be seen in our average MRI templates as well (Figure 4).

Some of these changes in GM and WM can be specifically linked to cognitive development (see Section 4). The dramatic changes in infancy in GM volume are primarily due to synaptogenesis and have concomitant changes in brain plasticity reflected in cognitive processes, memory, and language development. Similarly, rapidly myelinated regions are believed to correspond to rapid changes in inter-area communication critical for integrated neurological or behavioral functioning (Casey, Giedd, & Thomas, 2000; Deoni et al., 2011). The more gradual changes in the childhood years are very closely related to developing cognitive processes (e.g., see Casey et al., 2000). We do not know if the changes in GM and WM have specific parallels in behavior in adult development. The changes in adulthood are more gradual and thus would likely be linked more loosely to changes in cognitive processes. The gradual changes in WM/GM volume in adults likely do not correspond to the more dramatic brain–behavior relations found in adult pathologies. Brain changes in later adult development often include pathological brain development, which are closely related to declines in several cognitive areas (e.g., memory loss, senile dementia, Alzheimer’s Disease, Parkinson’s).

We focused in further on changes occurring during infancy. There are extremely rapid changes in WM volume in infancy due to rapid axonal myelination during this time. Changes in myelination in infants have been documented in several places (Conel, 1939–1967; Kinney et al., 1988, 1994; Yakovlev & Lecours, 1967). We have reviewed this topic previously (Richards, 2009). Myelin is a fatty substance that in adult brains covers the axons of many neurons. It appears “white” in autopsy slices; fatty tissue reflects light. The T1 relaxation time of the cells making up the myelinated sheath have a long T1 relaxation time compared to GM, CSF, bone, and other head tissue. Therefore, it appears as “bright voxels” in a

T1-weighted MRI volume (T1-weighted volumes are designed to maximally discriminate WM, GM, and OM). Any MRI volume of infant brains shows obvious lack of myelination in the first few months (see examples in Richards, 2009; Sanchez et al., 2011). This is obvious in our average MRI templates (Figure 3) and in our segmented priors (Figure 4).

The individual MRI volumes for infant participants were used to further examine changes in GM and WM. Recall that we have segmented MRI volumes with partial volume estimates for GM, WM, and OM for all of our infant participants, and lobar and stereotaxic atlases for infant participants and 2-, 3-, and 4-year-olds. We used the lobar segments to mask the GM and WM volumes for frontal, occipital, parietal, and temporal lobes. Figure 8 shows the segmented GM (top left panel) and WM (top right panel) separately for the four cortical lobes. The GM volume increased steadily in the frontal and temporal lobes across the entire age; the parietal lobe showed gradual increases in size through 4 years. The occipital lobe GM did not change appreciably during this age period.

Frontal lobe WM increased across ages in this analysis (Figure 10, top left panel). All four lobes showed increases in WM volume from birth through 4.5 months of age. However, WM volume for the occipital, parietal, and temporal lobes showed no reliable change from 4.5 through 12 months, whereas frontal lobe WM volume continued to increase during this time. The WM volume increased from 12 months through 4 years in frontal, parietal, and temporal lobes but appeared to have little change in the occipital lobe after 4 months. It should be noted that GM and WM volume changed significantly in the frontal lobes for all the reported age comparisons.

These findings advance our knowledge of human brain and head development across the life span. To our knowledge, this is the first analysis of

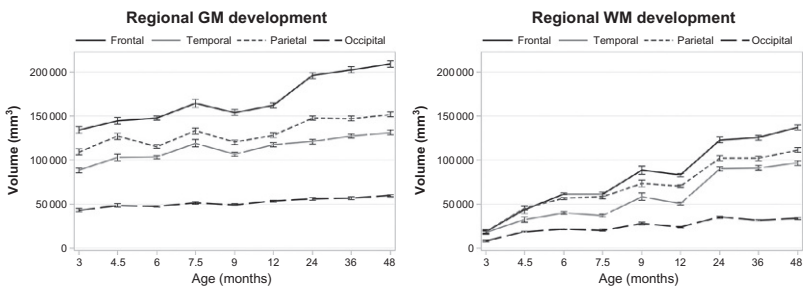


Figure 8 Gray matter- and white matter-segmented tissue volume in infants and preschool children as a function of scan age for the frontal, occipital, parietal, and temporal lobes. The error bars represent the standard error of the mean (SE).

MRI data from participants from 2 weeks to 89 years. We are missing only newborn participants! Our findings were consistent with previous reports that used participants from limited age ranges. The rapid development of total brain, GM, and WM volume during infancy found in our study was consistent with Knickmeyer et al. (2008) and other studies with infant participants. The inverted U-shape of GM and the linear increase pattern of WM throughout childhood and adolescence (Figure 9) agreed with previous reports with children and adolescents (e.g., Giedd et al., 1999; Lenroot et al., 2007). However, the development of GM shown in our study was inconsistent with some reports from the adult portion of the life span. Several reports have stated that the decline in GM volume begins about age 20 (e.g., Lemaître et al., 2005; Sullivan et al., 2004; Taki et al., 2004). Our findings suggested the peak in GM for the entire life span occurred in the late childhood or early adolescence, with decreases in GM volume across the rest of the life span. The OM measured in our study may represent the amount of CSF from infancy to childhood, but it likely contains increasing amounts of tissue other than CSF as adulthood progresses. The linear increase pattern of OM was consistent with previous findings for CSF development in adulthood (Good et al., 2001; Lemaître et al., 2005; Smith et al., 2007), which indicated that the OM development was highly associated with CSF change.

3.2. “Study-Specific” MRI Templates and Neurostructural Development in Chinese Children

It is clear from our work that the age-specific reference data are important due to differences among pediatric, young adult, and aging adult brains. There may be other factors that influence brain anatomical features. These could include gender, racial or ethnic status, developmental status, or children with atypical development (e.g., neurodevelopmental disorders). One example of this is with participants from different racial/ethnic backgrounds. Studies with MRI scans from adult participants have revealed morphological and structural differences between Asian and North American brains (Lee et al., 2005; Tang et al., 2010). For instance, Tang et al. (2010) compared brain morphological features (length, width, height, and AC–PC distance) between Chinese and U.S. adults. Chinese adult brains were found to be shorter, wider, and larger height than U.S. adult brains. Lee et al. (2005) provided similar differences between Korean and North American adult brains. Anatomical differences between Asian and North American brains are not limited to morphological features. Tang et al. (2010) conducted a

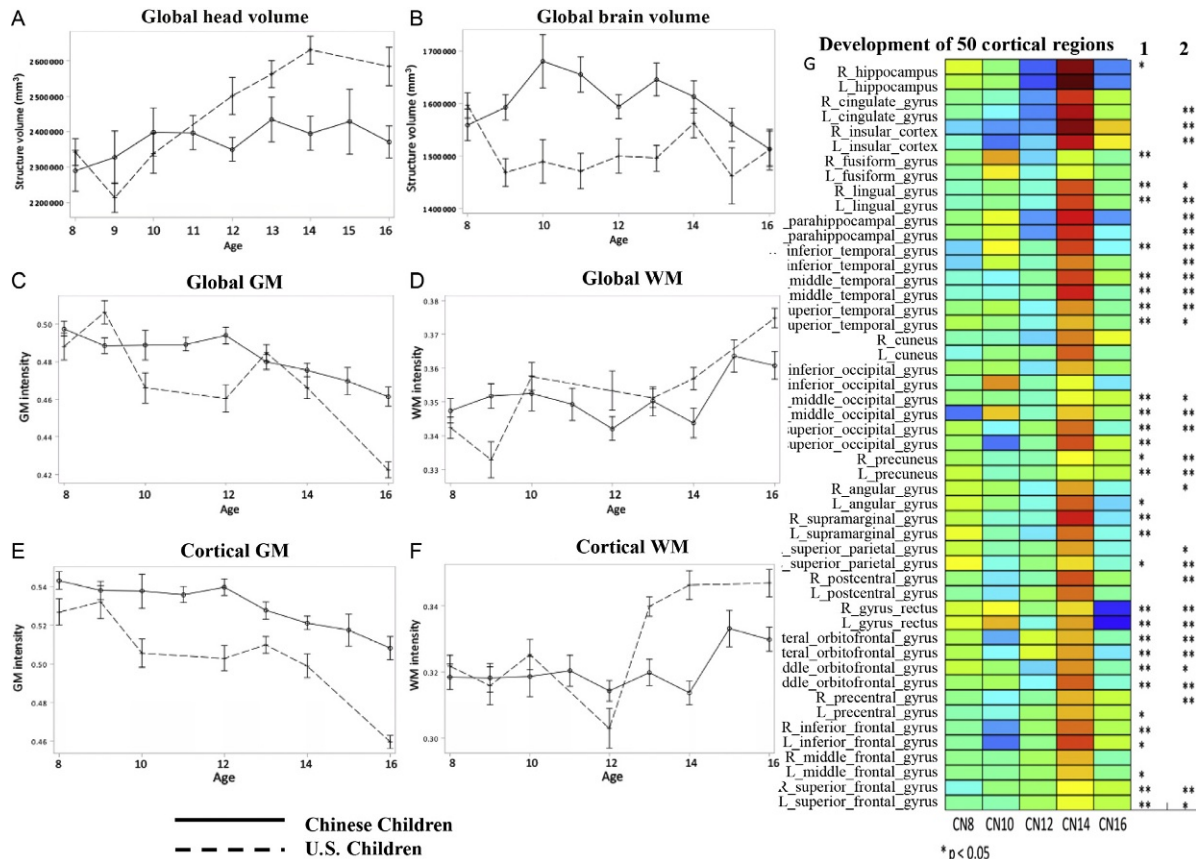


Figure 9 Head and brain development in Chinese and North American children. Panels (A–F) show changes in head, brain, GM, and WM volume from ages 8–16 for a group of Chinese children and individual participants selected from the Neurodevelopmental MRI Database. Panel (G) shows GM age patterns in 50 cortical regions for Chinese children. Each cell shows the ratio of GM volume in that regions for that age group to the average for all groups, with significant differences occurring primarily at age 14. Column 1 has asterisks representing a nationality main effect across the five age groups between Chinese and North American children. Column 2 shows parallel results for Chinese and North American adults found in [Tang et al. \(2010\)](#).

comparison of brain regional volume for 56 brain structures between the two populations. There were several differences in volume in a number of these brain structures (e.g., the left middle orbitofrontal gyrus, left gyrus rectus, and right insular cortex).

The differences between brain morphological features in Asian and North American adults suggest that nationality-appropriate reference data would be useful. This could reduce potential inaccurate deformation of MR images during image registration, and potential misclassification of brain tissue (with segmented priors) or brain regions (with stereotaxic atlases) caused by nationality-inappropriate reference volumes. To this end, [Lee et al. \(2005\)](#) and [Tang et al. \(2010\)](#) created the average MRI templates for Korean and Chinese adults, respectively. Measurements of these Asian templates indicated morphological differences compared to the ICBM-152 template. These Asian adult templates were found to be shorter but wider, and their heights were notably smaller than the ICBM-152 template. Validity tests in the [Tang et al. \(2010\)](#) study confirmed the hypothesis that using nationality inappropriate template (ICBM-152) would lead to significantly more deformations of MR images coming from Chinese adult participants.

Given the differences in brain morphology and regional distribution between Asian and North American adult participants, it could be expected that such differences were found in children. The patterns of brain development shown in the previous [Section 3.1](#) may be dissimilar in children from Asian backgrounds. Very few studies have examined possible differences between neurostructural developmental trajectories of Asian and North American populations. We know of only two studies that examined Chinese children and adolescent brain development ([Guo et al., 2007](#); [Guo, Jin, Chen, Peng, & Yao, 2008](#)). No study has directly compared neurostructural development between Chinese and North American pediatric participants.

We conducted a study to fill this gap by directly comparing brain development between Chinese and North American children and adolescents from 8 to 16 years ([Xie et al., 2014a, 2014b](#)). The MRI scans were collected from 133 (82 M, 51 F) Chinese children and adolescents from Sichuan province, China. These were 3T, 3D MRI scans with resolution similar to that done at the MCBI. The MRI data preparation and preliminary processing were performed using similar procedures to the participants in the Neurodevelopmental MRI Database (e.g., [Sanchez et al., 2011, 2012](#)). Age- and gender-matched children were selected from the database. We compared brain and head morphological changes, brain and head volume

development, GM and WM development, and volumetric changes in 50 cortical regions between Chinese and their North American counterparts.

There were several intriguing findings in this analysis. First, Chinese children and adolescents' brain and head were shorter, wider, and taller than their North American cohorts. Both groups showed a linear increase in brain/head length over these ages, with the North American children's head being about 5 mm longer than that of the Chinese children at the same age. Conversely, a similar pattern was found for changes in head width, but in this case, the average Chinese children head was about 5–7 mm wider than the North American children's head.

Second, brain and head volumes showed different developmental patterns for Chinese and North American children across these ages. [Figure 9](#) shows the results of the volumetric analysis of head and brain changes over age for these two groups. Overall, there were increases in head volume for both groups ([Figure 9A](#)), but the rate of change and eventual volume was larger in the North American children. For brain volume, the pattern was different. Chinese and North American children showed invert U-shape patterns in brain volume, with an earlier peak for Chinese children ([Figure 9B](#)). In addition, Chinese children were found to have a larger brain volume than North American children from about 9 to 15 years.

Third, we analyzed changes in GM and WM as a function of age. The pattern of change in GM and WM volume in both groups was similar to those found in our previous analysis. Overall, there was a gradual decline in total GM volume similar to those found in our prior analysis (cf. [Figure 9C](#) and [D](#) with [Figure 9A](#)). These patterns held when comparing cortical GM or WM over these ages, with some differences in overall volume between the two groups ([Figure 9E](#) and [F](#)). Finally, we used the LPBA40 ([Shattuck et al., 2008](#)) to mask regional volumes in the cortex separately for 50 brain regions (cf., [Tang et al., 2010](#)) and analyzed the volumes of those 50 regions. [Figure 9G](#) shows the volumetric changes in these regions for the Chinese children. Most of the brain regions showed increases in volume through 14 years and then decreases thereafter. An interesting comparison may be made between our results with children and those of [Tang et al. \(2010\)](#) with adults. The asterisks in [Figure 9](#) show differences between Chinese and North American children in our analysis (Column 1) and Chinese and North American adults in [Tang et al.'s](#) analysis (Column 2). We found a very similar pattern of results for the children in which regions showed differences as [Tang et al.](#) reported for adults.

There are several implications from these results. The regional volume differences in the 50 cortical regions found in adults were already dissociated in young children. This implies that these differences must exist before this period of childhood. Future work that examines the nationality effect on brain development in other ages will advance our understanding of these differences. These findings also suggest that morphological differences between these two groups could affect the use of standard age-appropriate reference data based on the templates we have created. This suggests that age-specific brain/head templates for Chinese children may reduce the deformations and misclassifications that would result from using templates constructed from populations that have these anatomical differences relative to Chinese children.

Given the differences between the Chinese and North American children found in this study, we felt it would be useful to create “study-specific” reference data for Chinese children. The data from the Chinese children were used to create age- and nationality-specific reference data (Xie et al., 2014a, 2014b). The data were grouped in five age groups in two-year increments (7–8, 9–10, 11–12, 13–14, and 15–16 years) to approximately match the age groups found in our 3T averages (Table 1). Average MRI templates and segmented priors (GM and WM) were constructed separately for head and brain for these ages. Figure 10 shows the average MRI templates from this work. Similar to our other templates (Figures 2 and 3), these average MRI templates have excellent resolution and show fine detail for both brain and head. These templates and segmenting priors are publicly available at our database (<http://jerlab.psych.sc.edu/neurodevelopmentalmriddatabase/chinesechildren>).

We tested whether these Chinese age-appropriate templates fit Chinese children MR images better than age-inappropriate (Chinese adult), nationality-inappropriate (North American children), and nationality- and age-inappropriate (North American young adult) templates. Both internal and external validity tests confirmed the fitness of our templates to Chinese children brain MR images. Using the Chinese age-appropriate templates as reference data for registration resulted in significantly less deformation of Chinese children MR images than using the templates from Chinese adults (Chinese 56, Tang et al., 2010), the U.S. age-specific children (Sanchez et al., 2012), or the North American adults (20–24 template from Sanchez et al., 2012). We suggest that these Chinese children brain and head MRI templates should be used in MRI research involving Chinese children and adolescents. These should reduce the potential misclassification of tissue

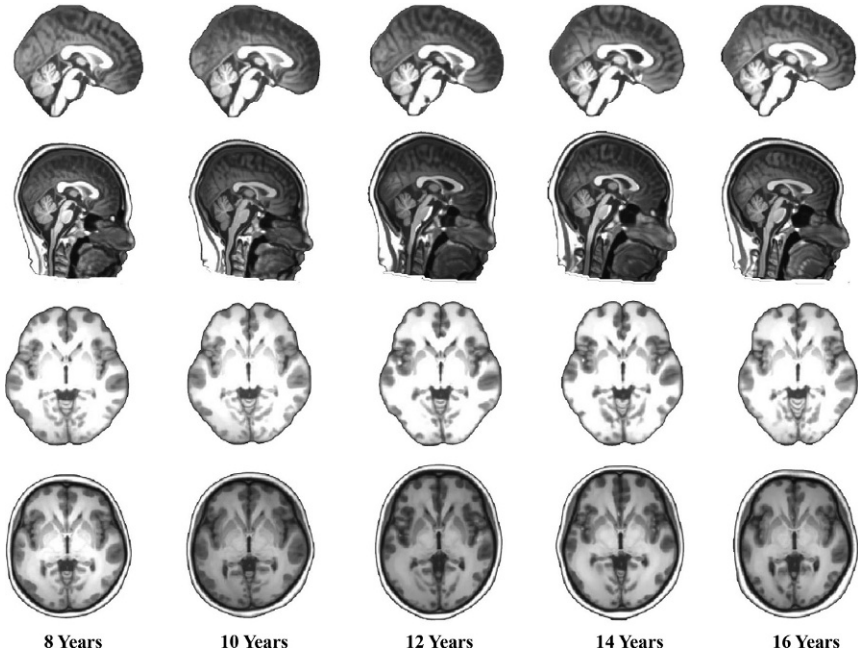


Figure 10 Brain and whole-head average MRI templates for Chinese children. The top two rows contain a midsagittal slice for brain and whole-head averages, and the bottom two rows show an axial slice at the level of the anterior commissure (AC). The figures from the different ages are shown as the same size, though they differ in size for the templates. The average MRI templates are oriented approximately with the MNI template.

types and deformations of MR images resulting from using age or nationality inappropriate references.

3.3. Nonmyelinated Axon Tissue Segmentation in Infants

Tissue segmentation of brain images from infants poses special challenges. The GM and WM contrast-to-noise ratio (CNR) for infant MRI is significantly lower than the CNR for adult brain MRI (Mewes et al., 2006). This results in poor resolution across the spatial aspects of the MRI volume and consequent difficulty in segmenting partial volume regions. During the first 2 years of life, the WM/GM contrast is reversed (as compared to adult contrast) on T1- and T2-weighted images and gradually changes toward the MRI contrast of adult brains (Leppert et al., 2009; Paus et al., 1999; Xue et al., 2007). At around 9 months of age, GM and WM demonstrate roughly the same intensities and cannot be segmented by the sole use of intensity

differentiation (Barkovich, 2005; Paus et al., 1999). Additionally, the brain in infants consists of a large amount of nonmyelinated axons (NMA). The T1 relaxation times for NMA and GM are approximately equivalent, so that “neuronal cell bodies” and “nonmyelinated axons” appear the same on T1W scans (e.g., Figures 2 and 3, youngest ages). Through the identification of myelinated and NMA, regional changes of WM and important maturational processes can be distinguished and quantified (Aubert-Broche, Fonov, Leppert, Pike, & Collins, 2008; Barkovich, 2005; Weisenfeld & Warfield, 2009). By about 2 years of age, the contrast found in the developing brain more closely resembles that of an adult brain due to the progression of increasing myelination and decreasing water content (Leppert et al., 2009; Rutherford, 2002).

Nonmyelinated and myelinated axons and cortical and subcortical GM have been analyzed separately in the neonatal brain (Anbeek et al., 2008; Hüppi et al., 1998; Prastawa et al., 2005; Weisenfeld & Warfield, 2009). The different tissue types in the infant brain exhibit significant levels of intensity inhomogeneity and variability, in addition to overlapping intensity distributions (Prastawa et al., 2005; Shi et al., 2010). Some researchers have developed methods to distinguish myelinated and NMA in MRIs. Prastawa et al. (2005) treated myelination as a fractional property, such that the MRI intensities reflected the degree of myelination in partial volume estimates. This procedure was somewhat successful in differentiating myelinated and NMA in the newborn brain. However, the dividing boundaries between the two tissue types were generally ambiguous (Prastawa et al., 2005; Rutherford, 2002), and the results showed mislabeled partial volume voxels (Xue et al., 2007). Others have expanded on the segmentation methodology of Prastawa et al. (2005) through the use of priors or iterative algorithms (Gilmore et al., 2007; Weisenfeld & Warfield, 2009). Hüppi et al. (1998) differentiated between myelinated and NMA in newborn brains and found a fivefold increase in the myelinated WM volume between 35 and 41 weeks postconception. Studies have demonstrated significant reductions (~35%) of myelination in preterm infants when compared to term infants (Inder, Warfield, Wang, Hüppi, & Volpe, 2005; Mewes et al., 2006). Neonatal studies showing early rapid developmental changes highlight the importance of delineating the complete progression of the myelination process.

We are working on procedures to create segmented priors for the reference data with GM, WM, CSF, OM, and NMA in the MRI volumes across infant age groups. Our segmentation technique uses both the T1W and T2W classification (Shi et al., 2010) to aid in tissue discrimination.

Myelinated axons appear as “white matter” in the T1W volumes and dark matter in T2W scans (adults, older children). NMA appear in the T2W volumes as slightly brighter intensity voxels than GM (young infants). [Figure 11](#) shows our procedure applied to two infants and the average MRI template for infants. The top row shows the identification of WM from the two-class model for a MRI from a 2-week-old participant. The two-class model categorizes WM successfully but classifies NMA with GM (top row, second column, blue (black in the print version) color). We then use the T2-weighted scan (third column) to identify the NMA (fourth column, green (gray in the print version) color) and create a three-class model (GM, WM, and NMA; far right column). [Figure 11](#) (second row) shows

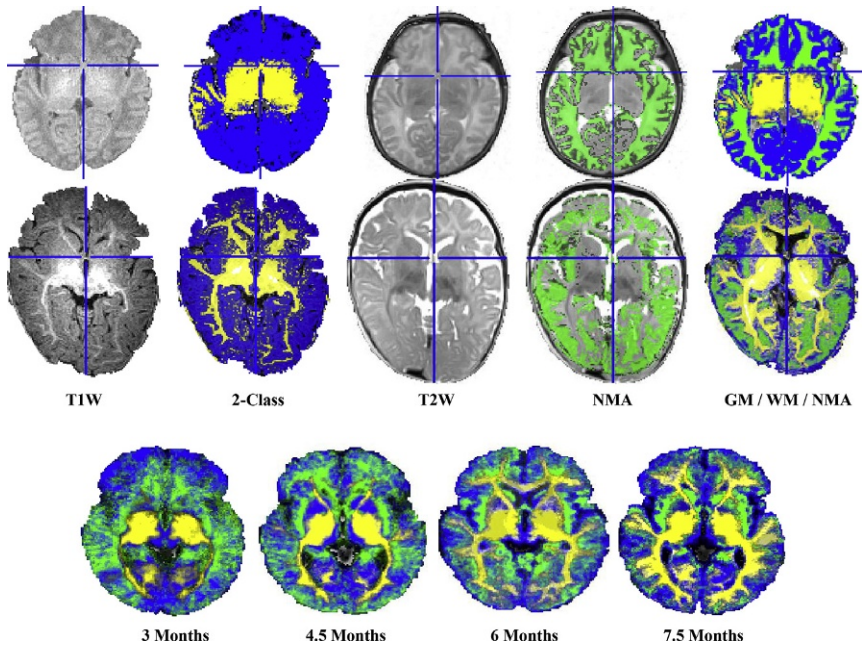


Figure 11 Axial slices demonstrating the NMA segmentation. The top and middle rows show the segmentation for a 2-week-old and 6-month-old, respectively. The columns from left to right are the T1W brain, “GM/WM” segmentation, the T2W and the NMA classified in the T2W, and the three-class segmentation (GM, WM, and NMA). The last row shows the change in the three-class model form 3 to 7.5 months for average MRI volumes and average probability values. The crosshairs on the coronal slices are centered on the anterior commissure. The brightness of the colors for the GM/WM and GM/WM/NMA represent the probability that the voxel belongs to the category (GM, blue (black in the print version); WM, yellow (white in the print version); NMA, green (gray in the print version)).

the results of this classification for a 6-month-old. Note the higher proportion of WM in the infant brain at this age. The third row shows the results of this analysis for the average MRI templates for infants ranging in age from 3 to 7.5 months of age.

We examined the changes in the NMA volume across the first year. The identification of GM with two-class models is compromised since NMA and GM are classified in the same category with the two-class (GM and WM) segmentation. So the changes in GM over age in the infancy period (e.g., Figure 8) overestimate the “gray matter” (neuron cell bodies, nuclei). Figure 12 shows a similar analysis of the tissue volumes for infants from 3 to 12 months. The changes in WM are the same as before, since myelinated axons are correctly identified with the two-class model. The GM in Figure 12 represents the GM (NMA) and NMA in the same figure. There is a change in volume of the NMA through the first 6 months, likely due to overall changes in axonal growth and synaptogenesis. However, this begins to drop by 7.5–9 months. This should decrease further in the second year.

The changes we report in WM volume are consistent with other reports, both from MRI analysis (Deoni et al., 2011) and other methods. The rapidly changing myelination likely affects integrated neurological or behavioral functions due to communication across different brain areas (Casey et al.,

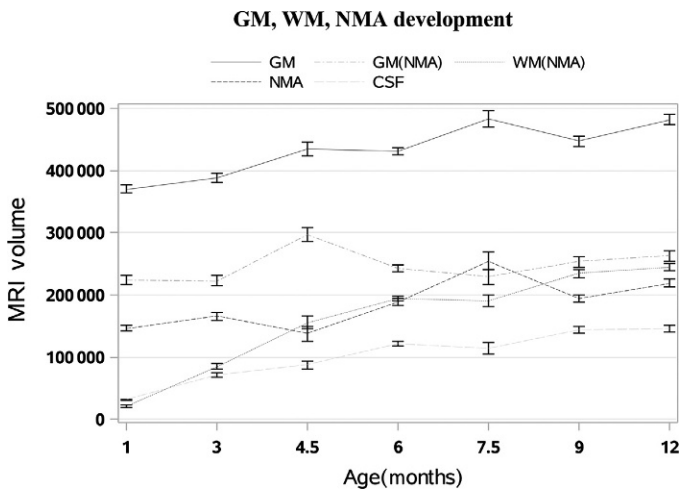


Figure 12 Gray matter, white matter, and nonmyelinated axons segmented tissue volume in infants as a function of age. The “GM” is from the GM/WM (OM) two-class segmentation, and the “GM (NMA)” is from the GM/NMA segmentation. The error bars represent the standard error of the mean (SE).

2000; Deoni et al., 2011). The results of the NMA volume analysis are new. Changes in GM volume have been interpreted as being primarily due to synaptogenesis. This should have a direct influence on behavioral plasticity during this age range as the emergence and pruning of synaptic connections results in learning, language development, memory, and developmental canalization. However, our analysis shows a more gradual increase in GM volume. The measurement of GM development in the first few months is confounded with volumetric increases in nonmyelinated axonal growth, whereas when axonal myelination is reflected in more WM there is an apparent increase in GM that actually reflects NMA decreases. We cannot specifically detail what GM–NMA–behavioral relations would occur with the distinction between GM and NMA, but our methods should result in a refined model of brain–behavior changes over this time period.

3.4. Contribution to Methods for Studying Brain Activity

One unique contribution of the “Neurodevelopmental MRI Database” is its applicability to the measurement of brain activity in pediatric populations. The quantitative analysis of brain function requires reference MRI volumes in order to normalize brain differences across participants (e.g., for fMRI analysis). Additionally, the study of brain activity with external measurement of scalp electrical activity (electroencephalogram (EEG) and ERP) requires age-appropriate scalp electrode measurement and age-appropriate head models. The “Neurodevelopmental MRI Database” is a unique resource for the study of such brain activity and should be useful in the study quantitative studies of developmental brain functioning. In this section, we will briefly review how this can be used to construct electrode placement locations and realistic head models for doing cortical source analysis of “event-related potentials” (ERPs) computed from the ongoing EEG of infants and young children. Second, we will mention two recent studies using the average MRIs to determine the probable generators of “near-infrared optical spectroscopy (NIRS)” recording on the scalp. [Table 2](#) has a list of several publications that have used this database for work in electrode placement, realistic head models for cortical source analysis, and for determining the cortical generators of NIRS locations.

The EEG is a measure of changing electrical activity on the scalp that is generated by neural activity. EEG is measured by placing recording electrodes on the head and measuring interelectrode electrical potential differences at each recording electrode. The electrical activity on the head is

Table 2 Example Uses of the Neurodevelopmental MRI Database for Measuring Brain Activity in Participants from 3 Months Through Adulthood

References	Age	Usage
<i>Electrode placement</i>		
Richards et al. (2014)	Young adults	Average electrodes for high-density recording
Near-infrared optical spectroscopy (NIRS)		
Emberson, Palmeri, Cannon, Richards, and Aslin (2013)	Infants and adults	Repetition suppression
Lloyd-Fox et al. (2013)	Infants	Action-perception and action processing
Lloyd-Fox et al. (2014)	Infants 4–7 months	Method for scalp projection
Papademetriou et al. (2013)	Infants 4–7 months	NIRS mapping for fMRI in infants
Richards (2014)	3–12 months	Method for scalp projection
Richards (2014)	2 years to adults	Method for scalp projection
<i>Realistic head models for cortical source analysis</i>		
Bathelt, O'Reilly, Clayden, Cross, and de Haan (2013)	2–5 years	Functional brain networks
Henderson, Luke, Schmidt, and Richards (2013)	Young adults	Brain activity during reading
McCleery and Richards (2012)	4.5–7.5 months	Comparing realistic and unrealistic head models
McCleery, Surtees, Graham, Richards, and Apperly (2011)	Young adults	Theory of mind
Reynolds, Courage, and Richards (2010)	4.5, 6, and 7.5 months	Visual preferences
Reynolds and Richards (2005)	4.5, 6, and 7.5 months	Familiarization and recognition memory
Richards (2005)	3, 4.5, and 6 months	Spatial cueing
Richards (2012)	3 and 4.5 months	Spatial cueing
Richards (2013a, 2013b)	Young adults	Antisaccades and prosaccades
Thorpe, Cannon, and Fox (2014)	1, 4 years, adults	Mu rhythm development
Zieber and Richards (2013)	4.5–7.5 months	Preference for mother face

generated by concurrent neural activity inside the head, probably coming from excitatory postsynaptic potentials (Reynolds & Richards, 2009). Therefore, EEG activity is a measure of brain activity recorded in real time. One use of EEG for studying functional brain activity is to synchronize the recording of the EEG with experimental events. Averages can then be made of the EEG activity at the onset of the event, i.e., “ERPs”. It is hypothesized that groups of neurons that are simultaneously active concurrent with the psychological processes surrounding the experiment stimulus event will produce electrical activity strong enough to be measured above the ongoing EEG. The relation between such ERPs activity (or ERP components) and behavior is the ability to produce a measure of functional brain activity that can serve as an important research tool for the field of cognitive neuroscience. EEG and ERP recording in pediatric populations has been an important tool because of the relative ease of use of the recording for infants and children, especially since other standard tools used in the study of adult brain activity are not as easily applied to younger participants.

The neurodevelopmental database can help in this enterprise in two fashions. First, accurate knowledge of the placement of the electrodes on the scalp of individual participants is helpful in localizing the scalp potentials to be analyzed. Reynolds and Richards (2005), for example, present a compelling case that both the number of electrodes and the placement of the electrodes on the scalp are important for localizing the ERP activity on the scalp. This is due both to the need to have full coverage of the head for analyzing brain activity and to have sufficient resolution to cover the known resolution of EEG/ERP activity. Recently, we developed tools for adult participants to place electrode locations on the scalp locations of a structural MRI from individual participants with electrode recordings and structural MRIs (Richards et al., 2014; see use in adults in Henderson et al., 2013; Richards, 2013a, 2013b; Table 2). We are now in a position to create accurate electrode placement locations on an average MRI template, or on individual participants. The individual participant electrode placements are done by having participants who have a structural MRI and an EEG recording session (Richards et al., 2014). We use fiducial measurements of the placement of the EEG recording electrodes on the infants head during the EEG recording and the same locations in the structural MRI volume to create a set of 3D positions in the MRI volume that correspond to each electrode location. Figure 13 shows an example of an EGI “HGSN-128” electrode net placement map for one individual (upper left panel). After gathering enough participants for a specific age, we can create

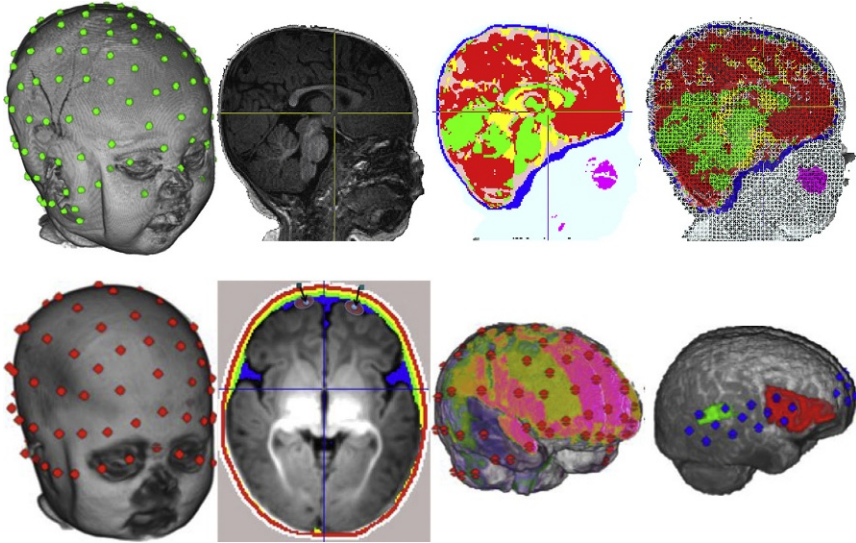


Figure 13 Examples of methods for individual participants brain activity measurement. Top row from left to right: EGI HGSN electrode recording locations on the 3D reconstruction of the head; midsagittal view of the T1-weighted scan; head segmentation in skin and muscle (white), gray matter (red (dark gray in the print version)), white matter (green (light gray in the print version)), CSF (cerebrospinal fluid, yellow (white in the print version)), dura (pink (gray in the print version)), skull (blue (black in the print version)), and nasal cavity (purple (dark gray in the print version)); representation of the finite element method tetrahedral wireframe used in EEG source analysis programs. Second row from left to right: 10–10 electrode recording locations on the 3D reconstruction of an average MRI template; illustration of projections from frontal scalp areas in toward prefrontal cortex; 10–10 electrode projections to cortical locations with Hammers stereotaxic atlas regions; NIRS projections from an NIRS holder onto an individual participant structural MRI, with the inferior frontal gyrus (red (gray in the print version)) and temporal–parietal junction (green (light gray in the print version)) “Regions of Interest.”

age-appropriate average electrode placement location map for the participants making up the average MRI template. These could be used by researchers who do not routinely use structural MRI for accurate placement maps. We also have the 10–10 electrode placements for each participant and for the average MRI templates (Figure 12, lower right panel). We have average electrode placements for a wide variety of ages (Table 2) (see recent use by Bathelt et al., 2013). The use of age-appropriate electrode placement maps should be extremely important in the accurate identification of scalp areas over which EEG and ERP activity occurs. This age-appropriate accuracy is critical when using electrode placements on realistic head models for ERP/EEG cortical source analysis (Reynolds & Richards, 2009).

A second way in which both structural recordings of participants and average MRI templates are becoming useful for EEG/ERP recording is in constructing realistic head models for cortical source analysis (see [Michel et al., 2004](#); [Reynolds & Richards, 2009](#); also [Richards, 2009](#); [Slotnick, 2004](#)). Cortical source analysis is a quantitative technique that takes the surface electrical recordings on the scalp (EEG or ERP) and localizes/quantifies the sources of the scalp electrical activity with generators located inside the head. This method is based on estimating the location and magnitude of electrical generators inside the head, which propagate current to the head through the various media of the head (e.g., GM, WM, CSF, skull, skin, muscle, and eyes). Accurate source analysis depends on having a realistic description of the materials inside the head ([Michel et al., 2004](#)). This is especially true for infant participants, whose head materials differ greatly from adult participants (e.g., GM, WM, and CSF) and whose brain topological arrangement substantially differs from adults ([Lew et al., 2013](#); [McCleery & Richards, 2012](#); [Reynolds & Richards, 2009](#); [Richards, 2009](#)). [Figure 13](#) shows the MRI from the infant photographed in [Figure 1](#). The middle section shows the materials identified in this infant, and the right figure shows a wireframe model that is used in computer programs for source analysis. Using realistic models of the head for source analysis may be especially important for very young children, where the topology, quantity, and type of head materials differs significantly from adult participants ([Lew et al., 2013](#); [Reynolds & Richards, 2005, 2009](#)). We are now in a position to accurately identify the materials inside the head and provide realistic models for participants of all ages. (For further information, see [Section 2](#), “What’s Inside a Baby’s Head,” [Richards, 2009](#).) Incidentally, the accurate identification of head models is also used in the analysis of “magnetoencephalogram” data. A similar approach to a realistic head model for 6-month-old infants is covered in [Akiyama et al. \(2013\)](#) (also see [Lew et al., 2013](#)). [Table 2](#) has a list of references using these procedures for cortical source analysis of EEG and ERP with realistic head models.

A third contribution of the Neurodevelopmental MRI Database to the measurement of brain activity in pediatric populations is recent work using average MRIs and individual participant MRIs to determine the probability of cortical generators of “NIRS” recording on the scalp. The NIRS is used to measure brain activity and has proved useful for pediatric populations ([Vanderwert & Nelson, 2014](#)). An infrared emitter placed on the scalp sends an infrared signal that penetrates several millimeters (2–3 cm) into the skull through to the cortex. Different wavelengths of light reflect off oxygenated and deoxygenated hemoglobin are measured at the scalp with a detector

placed near the emitter. This procedure is applied to infants routinely (Vanderwert & Nelson, 2014). It is standard practice to use the 10–10 recording system to standardize the regions of the scalp for sensor placement. These coordinates have been localized to underlying cortical areas for adult participants (Homan, Herman, & Purdy, 1987; Okamoto et al., 2004; Singh, Okamoto, Dan, Jurcak, & Dan, 2005; Tsuzuki et al., 2012, 2007). Recently, researchers have begun to coregister NIRS sensor positions located on the scalp with underlying cortical anatomy. However, these have been with standard brain space (Blume, Buza, & Okazaki, 1974), on a single infant (Matsui et al., 2014), or with a limited range of ages (Kabdebon et al., 2014).

Recently, the data from the Neurodevelopmental MRI Database were used to resolve this issue for infants (Richards, 2014). Methods were developed that measured both the 10–10 recording system electrode positions and the EGI HGSN and GSN positions on the scalp of individual infant participant structural MRIs. For example, Figure 13 (lower right panel) shows the location of the 10–10 electrode system on an average MRI. A line is then projected from the positions on the scalp inward until it reaches the cortex (Figure 13, second lower right panel). A line was then projected from this position on the scalp inward until it reached the cortex. Then the stereotaxic atlases (Section 2.4) were used to determine the cortical regions representing those voxels in the MRI. Figure 13 (third lower right panel) shows the 10–10 recording positions projected onto the cortex and the stereotaxic atlas regions for the Hammers atlas for this MRI. A comprehensive database of scalp-to-cortical anatomy was constructed for infants from 3 to 12 months of age. We are currently working on a similar database for children and adolescents based on the 3T MRI participant data and average MRI templates (Richards, 2014). We also applied this technique recently to a group of infant participants who had both a structural MRI and an NIRS recording (Lloyd-Fox et al., 2014). We were able to reconstruct the NIRS holder on the head of individual participants, do the inward cortical projection, and determine both cortical locations for the individual and “region-of-interest” methods for specific areas. Figure 13 (lower left panel) shows the results from one participant with the inferior frontal gyrus and temporal–parietal junction highlighted. Table 2 has a list of recent references using the Neurodevelopmental MRI Database in NIRS recordings in infants.



4. RELATION TO BRAIN-BEHAVIOR DEVELOPMENT

Section 2 presented the Neurodevelopmental MRI Database, and in Section 3, we showed how it could be applied to the study of neurostructural

development and measurement of brain activity. We have only briefly addressed the relation between brain development and behavior development. In the last two decades, there has been a growing interest in the relation between structural and functional changes in the developing human brain. In recent years, direct evidence has been shown for the effects of brain structural changes on cognitive development in pediatric populations. For instance, [Rice et al. \(2014\)](#) examined the role of amygdala in the development of theory of mind (i.e., mental state inferences) in children from 4 to 6 years. They looked at the relation between children amygdala MRI volume and children's performance on face-based and story-based false-belief tasks. They found that amygdala MRI volume was related to face-based mental state inference and that larger amygdala volume was related to better performance on face-based cognitive inference. This relation was not found in their adult control group.

Another study showing a close relation between brain structural development and behavior was conducted by [Fjell et al. \(2012\)](#). They addressed how brain structural maturation leads to improvement in self-regulation ability during childhood. The flanker task was employed to measure children's cognitive control. Structural MRI scans were used for the quantification of cortical thickness and surface area and DTI was used for quantification of the quality of the major fiber connections between brain regions. Their results showed that the surface area of the anterior cingulate cortex, which plays an important role in impulse control and attention in adults, explained a significant proportion of children's cognitive performance. In addition, properties of large fiber connections accounted for a certain amount of variance in self-regulation.

We do not know of studies that have used the Neurodevelopmental MRI Database to study structure–behavior relations directly. The studies listed in [Table 2](#) have used the database to advance the study of brain function development as it relates to behavioral and psychological development in pediatric and adult populations. We hope that future work will use the structural measurement capability of the database to examine structural development in individual participants and relate that development to measures of overt behavioral and psychological development. We believe the database will be extremely useful for such work.

ACKNOWLEDGMENTS

This research was supported by Grants from the National Institute of Child Health and Human Development, R37-HD18942.

The Chinese children MRIs were obtained from Qiyong Gong, Huaxi MR Research Center (HMRRC), Department of Radiology, West China Hospital of Sichuan University,

Chendong, Sichuan, China, whose work was supported by National Natural Science Foundation (Nos. 81030027, 81227002, and 81220108013) and National Key Technologies R&D Program (No. 2012BAI01B03) of China.

Paul Fillmore created Figure 5 based on his work with infant stereotaxic atlases for the average MRI templates (Fillmore, Richards, et al., 2014). Figures 8, 11, and 12 were adapted from preliminary analyses in work done by Sanchez et al. (2011) but were recalculated based on our infant and preschool atlases (Figure 11) and new data (Figures 8 and 12).

The MRIs for the Neurodevelopmental MRI Database came from several sources. First, locally collected data come from the McCausland Center for Brain Imaging (McCausland Center for Brain Imaging, MCBI (<http://www.mccauslandcenter.sc.edu>). This includes all the infant 3T MRI's, MRIs from children ranging from 6 to 18 years, and adult MRIs for participants from 18.5 through 34 years of age. Second, infant and child MRI were obtained from the NIH MRI Study of Normal Brain Development (NIHPD (http://www.bic.mni.mcgill.ca/nihpd/info/data_access.html). This includes 2D, 1.5T scans for infants and children from 2 weeks through 4 years of age (Objective 2) and 2D and 3D, 1.5T scans for children from 4.5 to 18 years of age (Objective 1), and some adult participants. Third, child data came from age- and gender-matched typically developing controls of the Autism Brain Imaging Data Exchange (ABIDE (Di Martino et al., 2013; http://fcon_1000.projects.nitrc.org/indi/abide/)). Fourth, adult data for participants from 20 to 89 years were obtained from the Information Extracted from Medical Images database (IXI: <http://biomedic.doc.ic.ac.uk/brain-development/index.php?n=Main.Datasets>). Finally, the Open Access Series of Imaging Studies (OASIS: <http://www.oasis-brains.org>) cross-sectional and longitudinal image sets were used for adults from 20 to 89 years of age.

REFERENCES

- Adolph, K. E., Gilmore, R. O., Freeman, C., Sanderson, P., & Millman, D. (2012). Toward open behavioral science. *Psychological Inquiry*, 23(3), 244–247.
- Akiyama, L. F., Richards, T. R., Imada, T., Dager, S. R., Wroblewski, L., & Kuhl, P. K. (2013). Age-specific average head template for typically developing 6-month-old infants. *PLoS One*, 8(9), e73821.
- Almli, C. R., Rivkin, M. J., & McKinstry, R. C. (2007). The NIH MRI study of normal brain development (objective-2): Newborns, infants, toddlers, and preschoolers. *NeuroImage*, 35(1), 308–325.
- Altay, M., Holland, S. K., Wilke, M., & Gaser, C. (2008). Infant brain probability templates for MRI segmentation and normalization. *NeuroImage*, 43, 721–730.
- Anbeek, P., Vincken, K. L., Groenendaal, F., Koeman, A., Van Osch, M. J., & Van der Grond, J. (2008). Probabilistic brain tissue segmentation in neonatal magnetic resonance imaging. *Pediatric Research*, 63(2), 158–163.
- Ashburner, J., & Friston, K. J. (2000). Voxel-based morphometry—The methods. *NeuroImage*, 11(6), 805–821.
- Aubert-Broche, B., Fonov, V., Leppert, I., Pike, G. B., & Collins, D. L. (2008). Human brain myelination from birth to 4.5 years. In *Medical Image Computing and Computer-Assisted Intervention—MICCAI 2008* (pp. 180–187). Berlin/Heidelberg: Springer.
- Avants, B. B., Epstein, C. L., Grossman, M., & Gee, J. C. (2008). Symmetric diffeomorphic image registration with cross-correlation: Evaluating automated labeling of elderly and neurodegenerative brain. *Medical Image Analysis*, 12(1), 26–41. <http://dx.doi.org/10.1016/j.media.2007.06.004>.

- Avants, B. B., Tustison, N. J., Song, G., Cook, P. A., Klein, A., & Gee, J. C. (2011). A reproducible evaluation of ANTs similarity metric performance in brain image registration. *NeuroImage*, *54*(3), 2033–2044.
- Barkovich, A. J. (2005). *Pediatric neuroimaging*. Philadelphia, PA: Lippincott Williams & Wilkins.
- Bathelt, J., O'Reilly, H., Clayden, J. D., Cross, J. H., & de Haan, M. (2013). Functional brain network organisation of children between 2 and 5 years derived from reconstructed activity of cortical sources of high-density EEG recordings. *NeuroImage*, *82*, 595–604.
- Blume, W. T., Buza, R. C., & Okazaki, H. (1974). Anatomic correlates of the ten–twenty electrode placement system in infants. *Electroencephalography and Clinical Neurophysiology*, *36*, 303–307.
- Bourgeois, J. P. (1997). Synaptogenesis, heterochrony and epigenesis in the mammalian neocortex. *Acta Paediatrica. Supplement*, *422*, 27–33.
- Brain Development Cooperative Group. (2006). The NIH MRI study of normal brain development. *NeuroImage*, *30*(1), 184–202.
- Brain Development Cooperative Group. (2012). Total and regional brain volumes in a population-based normative sample from 4 to 18 years: The NIH MRI study of normal brain development. *Cerebral Cortex*, *22*(1), 1–12.
- Braver, T. S., Cohen, J. D., Nystrom, L. E., Jonides, J., Smith, E. E., & Noll, D. C. (1997). A parametric study of prefrontal cortex involvement in human working memory. *NeuroImage*, *5*, 49–62.
- Brunner, P., & Ernst, R. R. (1979). Sensitivity and performance time in NMR imaging. *Journal of Magnetic Resonance* (1969), *33*(1), 83–106.
- Burgund, E. D., Kang, H. C., Kelly, J. E., Buckner, R. L., Snyder, A. Z., Petersen, S. E., et al. (2002). The feasibility of a common stereotactic space for children and adults in fMRI studies of development. *NeuroImage*, *17*(1), 184–200.
- Byars, A. W., Holland, S. K., Strawsburg, R. H., Bommer, W., Dunn, R. S., Schmithorst, V. J., et al. (2002). Practical aspects of conducting large-scale functional magnetic resonance imaging studies in children. *Journal of Child Neurology*, *17*(12), 885–889.
- Casey, B. J., Cohen, J. D., Jezzard, P., Turner, R., Noll, D. C., Trainor, R. J., et al. (1995). Activation of prefrontal cortex in children during a nonspatial working memory task with functional MRI. *NeuroImage*, *2*, 221–229.
- Casey, B. J., Cohen, J. D., O'Craven, K., Davidson, R., Irwin, W., Nelson, C. A., et al. (1998). Reproducibility of fMRI results across four institutions using a working memory task. *NeuroImage*, *8*, 249–261.
- Casey, B. J., Giedd, J. N., & Thomas, K. M. (2000). Structural and functional brain development and its relation to cognitive development. *Biological Psychology*, *54*(1), 241–257.
- Casey, B. J., Trainor, R. J., Orendi, J. L., Schubert, A. B., Nystrom, L. E., Giedd, J. N., et al. (1997). A developmental functional MRI study of prefrontal activation during performance of a go-no-go task. *Journal of Cognitive Neuroscience*, *9*(6), 835–847.
- Collins, D. L., Neelin, P., Peters, T. M., & Evans, A. C. (1994). Automatic 3D intersubject registration of MR volumetric data into standardized Talairach space. *Journal of Computer Assisted Tomography*, *18*, 192–205.
- Conel, J. L. (1939–1967). *Postnatal development of the human cerebral cortex* (Vols. 1–8). Cambridge, MA: Harvard University Press.
- Deoni, S. C., Mercure, E., Blasi, A., Gasston, D., Thomson, A., Johnson, M., et al. (2011). Mapping infant brain myelination with magnetic resonance imaging. *Journal of Neuroscience*, *31*(2), 784–791.
- Desikan, R. S., Segonne, F., Fischl, B., Quinn, B. T., Dickerson, B. C., Blacker, D., et al. (2006). An automated labeling system for subdividing the human cerebral cortex on MRI scans into gyral based regions of interest. *NeuroImage*, *31*(3), 968–980.

- Di Martino, A., Yan, C. G., Li, Q., Denio, E., Castellanos, F. X., Alaerts, K., et al. (2013). The autism brain imaging data exchange: Towards a large-scale evaluation of the intrinsic brain architecture in autism. *Molecular Psychiatry*, 19(6), 659–667. <http://dx.doi.org/10.1038/mp.2013.78>.
- Emberson, L., Palmeri, H., Cannon, G., Richards, J. E., & Aslin, R. N. (2013). *Differences in repetition suppression across sensory systems in 6-month-olds: Using NIRS to compare infant and adult neural function*. Poster presented at the Cognitive Neuroscience Society, San Francisco, April 2013.
- Ericsson, A., Aljabar, P., & Rueckert, D. (2008). Construction of a patient-specific atlas of the brain: Application to normal aging. In *ISBI* (pp. 480–483): IEEE.
- Evans, A. C. (2005). Large-scale morphometric analysis of neuroanatomy and neuropathology. *Anatomy and Embryology*, 210(5–6), 439–446.
- Evans, A. C., Brown, E., Kelly, R. L., & Peters, T. (1994). *3D statistical neuroanatomical models from 305 MRI volumes*. Piscataway, NJ: IEEE.
- Evans, A. C., Collins, D. L., Mills, S. L., Brown, E. D., Kelly, R. L., & Peters, T. M. (1993). 3D statistical neuroanatomical models from 305 MRI volumes. In *Proceedings of the IEEE-nuclear science symposium and medical imaging conference* (pp. 1813–1817).
- Evans, A. C., Collins, D. L., & Milner, B. (1992). An MRI-based stereotaxic atlas from 250 young normal subjects. *Journal of the Society for Neuroscience. Abstracts*, 18, 408.
- Fan, Y., Shi, F., Smith, J. K., Lin, W., Gilmore, J. H., & Shen, D. (2011). Brain anatomical networks in early human brain development. *NeuroImage*, 54(3), 1862–1871.
- Fillmore, P., Phillips-Meek, M., & Richards, J. (2014). Age-specific MRI brain and head templates for healthy adults from 20 through 89 years of age. Unpublished manuscript, submitted for publication.
- Fillmore, P., Richards, J. E., Phillips-Meek, M. C., Cryer, A., & Stevens, M. (2014). Stereotaxic MRI brain atlases for infants from 3 to 12 months. Unpublished manuscript, submitted for publication.
- Fjell, A. M., Walhovd, K. B., Brown, T. T., Kuperman, J. M., Chung, Y., Hagler, D. J., et al. (2012). Multimodal imaging of the self-regulating developing brain. *Proceedings of the National Academy of Sciences of the United States of America*, 109(48), 19620–19625.
- Fonov, V., Evans, A. C., Botteron, K., Almli, C. R., McKinstry, R. C., & Collins, D. L. (2011). Unbiased average age-appropriate atlases for pediatric studies. *NeuroImage*, 54, 313–327.
- Fotinos, A. F. S., Snyder, A. Z. P. M. D., Girton, L. E. B., Morris, J. C. M., & Buckner, R. L. P. (2005). Normative estimates of cross-sectional and longitudinal brain volume decline in aging and AD. *Neurology*, 64(6), 1032–1039.
- Fox, M., & Uecker, A. (2005). *Talairach daemon client*. San Antonio, TX: University of Texas Health Sciences Center. <http://ric.uthscsa.edu/projects/talairachdaemon.html>.
- Gao, W., Zhu, H., Giovanello, K. S., Smith, J. K., Shen, D., Gilmore, J. H., et al. (2009). Evidence on the emergence of the brain's default network from 2-week-old to 2-year-old healthy pediatric subjects. *Proceedings of the National Academy of Sciences of the United States of America*, 106(16), 6790–6795.
- Ge, Y., Grossman, R. I., Babb, J. S., Rabin, M. L., Mannon, L. J., & Kolson, D. L. (2002). Age-related total gray matter and white matter changes in normal adult brain. Part I: Volumetric MR imaging analysis. *AJNR. American Journal of Neuroradiology*, 23(8), 1327–1333.
- Giedd, J. N., Blumenthal, J., Jeffries, N. O., Castellanos, F. X., Liu, H., Zijdenbos, A., et al. (1999). Brain development during childhood and adolescence: A longitudinal MRI study. *Nature Neuroscience*, 2(10), 861–863. <http://dx.doi.org/10.1038/13158>.
- Giedd, J. N., Vaituzis, A. C., Hamburger, S. D., Lange, N., Rajapakse, J. C., Kaysen, D., et al. (1996). Quantitative MRI of the temporal lobe, amygdala, and hippocampus in

- normal human development: Ages 4–18 years. *Journal of Comparative Neurology*, 366(2), 223–230.
- Gilmore, J. H., Lin, W., Prastawa, M. W., Looney, C. B., Vetsa, Y. S., Knickmeyer, R. C., et al. (2007). Regional gray matter growth, sexual dimorphism, and cerebral asymmetry in the neonatal brain. *Journal of Neuroscience*, 27(6), 1255–1260.
- Gogtay, N., Giedd, J. N., Lusk, L., Hayashi, K. M., Greenstein, D., Vaituzis, A. C., et al. (2004). Dynamic mapping of human cortical development during childhood through early adulthood. *Proceedings of the National Academy of Sciences of the United States of America*, 101(21), 8174–8179.
- Good, C. D., Johnsrude, I. S., Ashburner, J., Henson, R. N. A., Friston, K. J., & Frackowiak, R. S. J. (2001). A voxel-based morphometric study of ageing in 465 normal adult human brains. *NeuroImage*, 14(1), 21–36.
- Gousias, I. S., Rueckert, D., Heckemann, R. A., Dyet, L. E., Boardman, J. P., Edwards, A. D., et al. (2008). Automatic segmentation of brain MRIs of 2-year-olds into 83 regions of interest. *NeuroImage*, 40(2), 672–684.
- Guimond, A., Meunier, J., & Thirion, J. P. (2000). Average brain model: A convergence study. *Computer Vision and Image Understanding*, 77, 192–210.
- Guo, X., Chen, C., Chen, K., Jin, Z., Peng, D., & Yao, L. (2007). Brain development in Chinese children and adolescents: A structural MRI study. *Neuroreport*, 18(9), 875–880. <http://dx.doi.org/10.1097/WNR.0b013e328152777e>.
- Guo, X., Jin, Z., Chen, K., Peng, D., & Yao, L. (2008). Gender differences in brain development in Chinese children and adolescents: A structural MRI study. *Proceedings of SPIE Medical Imaging*, 6916, 1–11.
- Hammers, A., Allom, R., Koeppe, M. J., Free, S. L., Myers, R., Lemieux, L., et al. (2003). Three-dimensional maximum probability atlas of the human brain, with particular reference to the temporal lobe. *Human Brain Mapping*, 19(4), 224–247.
- Heckemann, R. A., Hajnal, J. V., Aljabar, P., Rueckert, D., & Hammers, A. (2006). Automatic anatomical brain MRI segmentation combining label propagation and decision fusion. *NeuroImage*, 33(1), 115–126.
- Heckemann, R. A., Hartkens, T., Leung, K., Hill, D. L. G., Hajnal, J. V., & Rueckert, D. (2003). Information extraction from medical images (IXI): Developing an e-Science application based on the globus toolkit. In *Proceedings of the 2nd UK e-Science All Hands Meeting, Nottingham, UK*.
- Henderson, J. M., Luke, S. G., Schmidt, J., & Richards, J. E. (2013). Co-registration of eye movements and event-related potentials in connected-text paragraph reading. *Frontiers in Systems Neuroscience*, 7, 28.
- Hoeksma, M. R., Kenemans, J. L., Kemner, C., & van Engeland, H. (2005). Variability in spatial normalization of pediatric and adult brain images. *Clinical Neurophysiology*, 116(5), 1188–1194.
- Homan, R. W., Herman, J., & Purdy, P. (1987). Cerebral location of international 10–20 system electrode placement. *Electroencephalography and Clinical Neurophysiology*, 66, 376–382.
- Huang, C. M., Lee, S. H., Hsiao, I. T., Kuan, W. C., Wai, Y. Y., Ko, H. J., et al. (2010). Study-specific EPI template improves group analysis in functional MRI of young and older adults. *Journal of Neuroscience Methods*, 189(2), 257–266.
- Huettel, S. A., Song, A. W., & McCarthy, G. (2004). *Functional magnetic resonance imaging: Vol. 1*. Sunderland, MA: Sinauer Associates.
- Hüppi, P. S., Warfield, S., Kikinis, R., Barnes, P. D., Zientara, G. P., Jolesz, F. A., et al. (1998). Quantitative magnetic resonance imaging of brain development in premature and mature newborns. *Annals of Neurology*, 43(2), 224–235.
- Huttenlocher, P. R. (1990). Morphometric study of human cerebral cortex development. *Neuropsychologia*, 28, 517–527.

- Huttenlocher, P. R. (1994). Synaptogenesis, synapse elimination, and neural plasticity in human cerebral cortex. In C. A. Nelson (Ed.), *Threats to optimal development, the Minnesota symposia on child psychology: Vol. 27* (pp. 35–54). Hillsdale, NJ: Lawrence Erlbaum.
- Inder, T. E., Warfield, S. K., Wang, H., Hüppi, P. S., & Volpe, J. J. (2005). Abnormal cerebral structure is present at term in premature infants. *Pediatrics*, *115*(2), 286–294.
- Jernigan, T. L., Archibald, S. L., Berhow, M. T., Sowell, E. R., Foster, D. S., & Hesselink, J. R. (1991). Cerebral structure on MRI. Part I: Localization of age-related changes. *Biological Psychiatry*, *29*(1), 55–67.
- Joshi, S., Davis, B., Jomier, M., & Gerig, G. (2004). Unbiased diffeomorphic atlas construction for computational anatomy. *NeuroImage*, *23*, S151–S160.
- Kabdebon, C., Leroy, F., Simonnet, H., Perrot, M., Dubois, J., & Dehaene-Lambertz, G. (2014). Anatomical correlations of the international 10–20 sensor placement system in infants. *NeuroImage*, *99*(1), 342–356.
- Kang, H. C., Burgund, E. D., Lugar, H. M., Petersen, S. E., & Schlaggar, B. L. (2003). Comparison of functional activation foci in children and adults using a common stereotactic space. *NeuroImage*, *19*(1), 16–28.
- Kinney, H., Brody, B., Kroman, A., & Gilles, F. (1988). Sequence of central nervous myelination in human infancy: Pattern of myelination in autopsied infants. *Journal of Neuropathology and Experimental Neurology*, *47*, 217–234.
- Kinney, H., Karthigasan, J., Borenshteyn, N., Flax, J., & Kirschner, D. (1994). Myelination in the developing human brain: Biochemical correlates. *Neurochemical Research*, *19*, 983–996.
- Knickmeyer, R. C., Gouttard, S., Kang, C., Evans, D., Wilber, K., Smith, J. K., et al. (2008). A structural MRI study of human brain development from birth to 2 years. *Journal of Neuroscience*, *28*(47), 12176–12182.
- Lancaster, J. L., Summerlin, J. L., Rainey, L., Freitas, C. S., & Fox, P. T. (1997). The Talairach Daemon, a database server for Talairach atlas labels. *NeuroImage*, *5*, S633.
- Lancaster, J. L., Woldorff, M. G., Parsons, L. M., Liotti, M., Freitas, C. S., Rainey, L., et al. (2000). Automated Talairach atlas labels for functional brain mapping. *Human Brain Mapping*, *10*, 120–131.
- Lange, N., Froimowitz, M. P., Bigler, E. D., Lainhart, J. E., & Brain Development Cooperative Group. (2010). Associations between IQ, total and regional brain volumes, and demography in a large normative sample of healthy children and adolescents. *Developmental Neuropsychology*, *35*(3), 296–317.
- Lee, J. S., Lee, D. S., Kim, J., Kim, Y. K., Kang, E., Kang, K. W., et al. (2005). Development of Korean standard brain templates. *Journal of Korean Medical Science*, *20*, 483–488.
- Lemaître, H., Crivello, F., Grassiot, B., Alperovitch, A., Tzourio, C., & Mazoyer, B. (2005). Age- and sex-related effects on the neuroanatomy of healthy elderly. *NeuroImage*, *26*(3), 900–911.
- Lenroot, R. K., & Giedd, J. N. (2006). Brain development in children and adolescents: Insights from anatomical magnetic resonance imaging. *Neuroscience and Biobehavioral Reviews*, *30*(6), 718–729.
- Lenroot, R. K., Gogtay, N., Greenstein, D. K., Wells, E. M., Wallace, G. L., & Giedd, J. N. (2007). Sexual dimorphism of brain development trajectories during childhood and adolescents. *NeuroImage*, *36*(4), 1065–1073.
- Leppert, I. R., Almlí, C. R., McKinstry, R. C., Mulkern, R. V., Pierpaoli, C., Rivkin, M. J., et al. (2009). T2 relaxometry of normal pediatric brain development. *Journal of Magnetic Resonance Imaging*, *29*(2), 258–267.
- Lew, S., Sliva, D. D., Choe, M. S., Grant, P. E., Okada, Y., Wolters, C. H., et al. (2013). Effects of sutures and fontanels on MEG and EEG source analysis in a realistic infant head model. *NeuroImage*, *76*, 282–293.

- Lloyd-Fox, S., Richards, J. E., Blasi, A., Murphy, D., Elwell, C. E., & Johnson, M. H. (2014). Co-registering NIRS with underlying cortical areas in infants. *Neurophotonics*, *1*(2), 020901.
- Lloyd-Fox, S., Wu, R., Richards, J. E., Elwell, C. E., & Johnson, M. H. (2013). Cortical activation to action perception is associated with action production abilities in young infants. *Cerebral Cortex*, bht207. <http://dx.doi.org/10.1093/cercor/bht207>.
- Mandal, P. K., Mahajan, R., & Dinov, I. D. (2012). Structural brain atlases: Design, rationale, and applications in normal and pathological cohorts. *Journal of Alzheimer's Disease*, *31*, 1–20.
- Marcus, D. S., Fotenos, A. F., Csernansky, J. G., Morris, J. C., & Buckner, R. L. (2010). Open access series of imaging studies: Longitudinal MRI data in nondemented and demented older adults. *Journal of Cognitive Neuroscience*, *22*(12), 2677–2684.
- Marcus, D. S., Wang, T. H., Parker, J., Csernansky, J. G., Morris, J. C., & Buckner, R. L. (2007). Open access series of imaging studies (OASIS): Cross-sectional MRI data in young, middle aged, nondemented, and demented older adults. *Journal of Cognitive Neuroscience*, *19*(9), 1498–1507.
- Matsui, M., Homae, F., Tsuzuki, D., Watanabe, H., Katagiri, M., Uda, S., et al. (2014). Referential framework for transcranial anatomical correspondence for fNIRS based on manually traced sulci and gyri of an infant brain. *Neuroscience Research*, *80*, 55–68.
- Mazziotta, J. C., Toga, A. W., Evans, A., Fox, P., & Lancaster, J. (1995). A probabilistic atlas of the human brain: Theory and rationale for its development. *NeuroImage*, *2*, 89–101.
- Mazziotta, J., Toga, A., Evans, A., Fox, P., Lancaster, J., Zilles, K., et al. (2001). A probabilistic atlas and reference system for the human brain: International Consortium for Brain Mapping (ICBM). *Philosophical Transactions of the Royal Society of London. Series B, Biological Sciences*, *356*(1412), 1293–1322.
- McCleery, J. P., & Richards, J. E. (2012). Comparing realistic head models for cortical source localization of infant event-related potentials. *Developmental Medicine and Child Neurology*, *54*(Suppl. 2), 10, abstract.
- McCleery, J. P., Surtees, A., Graham, K. A., Richards, J. E., & Apperly, I. A. (2011). The neural and cognitive time-course of theory of mind. *Journal of Neuroscience*, *31*, 12849–12854.
- Mewes, A. U., Hueppi, P. S., Als, H., Rybicki, F. J., Inder, T. E., McAnulty, G. B., et al. (2006). Regional brain development in serial magnetic resonance imaging of low-risk preterm infants. *Pediatrics*, *118*(1), 23–33.
- Michel, C. M., Murray, M. M., Lantz, G., Gonzalez, S., Spinelli, L., & Grave de Peralta, R. (2004). EEG source imaging. *Clinical Neurophysiology*, *115*(10), 2195–2222.
- Muzik, O., Chugani, D. C., Juhasz, C., Shen, C. G., & Chugani, H. T. (2000). Statistical parametric mapping: Assessment of application in children. *NeuroImage*, *12*(5), 538–549.
- NIH. (1998). *Pediatric study centers (PSC) for a MRI study of normal brain development*. NIH RFP NIH/NINDS- 98-13, sponsored by National Institute of Neurological Disorders and Stroke, National Institute of Mental Health, National Institute of Child Health and Human Development.
- Okamoto, M., Dan, H., Sakamoto, K., Takeo, K., Shimizu, K., Kohno, S., et al. (2004). Three-dimensional probabilistic anatomical cranio-cerebral correlation via the international 10–20 system oriented for transcranial functional brain mapping. *NeuroImage*, *21*(1), 99–111.
- Papademetriou, M. D., Richards, J. E., Correia, T., Blasi, A., Lloyd-fox, S., Johnson, M., et al. (2013). Cortical mapping of 3D optical topography in infants. *Advances in Experimental Medicine and Biology*, *985*, 455–461.
- Paus, T., Zijdenbos, A., Worsley, K., Collins, D. L., Blumenthal, J., Giedd, J. N., et al. (1999). Structural maturation of neural pathways in children and adolescents: In vivo study. *Science*, *283*(5409), 1908–1911.

- Penny, W., Friston, K., Ashburner, J., Keibel, S., & Nichols, J. (2007). *Statistical parametric mapping: The analysis of functional brain images*. New York: Academic Press.
- Phillips, M. C., Richards, J. E., Stevens, M., & Connington, A. (2013). *A stereotaxic MRI brain atlas for infant participants*. In Paper presented at the SRCD, Seattle, WA, April 2013. <http://jerlab.psych.sc.edu/richardsinfo/conferencepresentations.php>.
- Prastawa, M., Gilmore, J. H., Lin, W., & Gerig, G. (2005). Automatic segmentation of MR images of the developing newborn brain. *Medical Image Analysis, 9*, 457–466.
- Reynolds, G. D., Courage, M. L., & Richards, J. E. (2010). Infant attention and visual preferences: Converging evidence from behavior, event-related potentials, and cortical source localization. *Developmental Psychology, 46*, 886–904.
- Reynolds, G. D., & Richards, J. E. (2005). Familiarization, attention, and recognition memory in infancy: An ERP and cortical source localization study. *Developmental Psychology, 41*, 598–615.
- Reynolds, G., & Richards, J. (2009). Cortical source localization of infant cognition. *Developmental Neuropsychology, 3*, 312–329.
- Rice, K., Viscomi, B., Riggins, T., & Redcay, E. (2014). Amygdala volume linked to individual differences in mental state inference in early childhood and adulthood. *Developmental Cognitive Neuroscience, 8*, 153–163.
- Richards, J. E. (2005). Localizing cortical sources of event-related potentials in infants' covert orienting. *Developmental Science, 8*(3), 255–278.
- Richards, J. E. (2009). Attention in the brain and early infancy. *Neoconstructivism: The new science of cognitive development: Vol. 1*. New York, NY: Oxford University Press.
- Richards, J. E. (2012). Cortical source analysis of ERP in infant spatial cueing. In Poster presented at the international conference on infant studies, Minneapolis, MN, June 2012.
- Richards, J. E. (2013a). Cortical sources of ERP in the prosaccade and antisaccade eye movements using realistic source models. *Frontiers in Systems Neuroscience, 7*, 27. <http://dx.doi.org/10.3389/fnsys.2013.00027>.
- Richards, J. E. (2013b). Cortical source analysis of ERP in infant spatial cueing. In Poster presented at the society for research in child development, Seattle, WA, April 2013.
- Richards, J. E. (2014). Scalp locations projected to cortical anatomy for infant NIRS. In Poster presented at the international conference on infant studies, Berlin, Germany, July 2014.
- Richards, J. E., Boswell, C., Stevens, M., & Vendemia, J. M. (2014). Evaluating methods for constructing average high-density electrode positions. *Brain Topography, 1*–17.
- Rutherford, M. A. (2002). *MRI of the neonatal brain*. London, UK: W. B. Saunders Co.
- Salat, D. H., Greve, D. N., Pacheco, J. L., Quinn, B. T., Helmer, K. G., Buckner, R. L., et al. (2009). Regional white matter volume differences in nondemented aging and Alzheimer's disease. *Neuroimage, 44*(4), 1247–1258.
- Sanchez, C., Richards, J., & Almlí, C. R. (2011). Neurodevelopmental MRI brain templates for children from 2 weeks to 4 years of age. *Developmental Psychology, 54*, 77–91.
- Sanchez, C., Richards, J., & Almlí, C. R. (2012). Age-specific MRI templates for pediatric neuroimaging. *Developmental Neuropsychology, 37*(5), 379–399.
- Sato, K., Taki, Y., Fukuda, H., & Kawashima, R. (2003). Neuroanatomical database of normal Japanese brains. *Neural Networks, 16*(9), 1301–1310.
- Shattuck, D. W., Mirza, M., Adisetiyo, V., Hojatkashani, C., Salamon, G., Narr, K. L., et al. (2008). Construction of a 3D probabilistic atlas of human cortical structures. *NeuroImage, 39*(3), 1064–1080.
- Shi, F., Fan, Y., Tang, S., Gilmore, J. H., Lin, W. L., & Shen, D. G. (2010). Neonatal brain image segmentation in longitudinal MRI studies. *NeuroImage, 49*(1), 391–400.
- Shi, F., Yap, P. T., Wu, G., Jia, H., Gilmore, J. H., Lin, W., et al. (2011). Infant brain atlases from neonates and 1- and 2-year-olds. *PLoS One, 6*(4), e18746.

- Singh, A. K., Okamoto, M., Dan, H., Jurcak, V., & Dan, I. (2005). Spatial registration of multichannel multi-subject fNIRS data to MNI space without MRI. *NeuroImage*, *27*, 842–851.
- Slotnick, S. D. (2004). Source localization of ERP generators. In T. C. Hardy (Ed.), *Event-related potentials: A methods handbook* (pp. 149–166). Cambridge: The MIT Press.
- Smith, C. D., Chebrolu, H., Wekstein, D. R., Schmitt, F. A., & Markesbery, W. R. (2007). Age and gender effects on human brain anatomy: A voxel-based morphometric study in healthy elderly. *Neurobiology of Aging*, *28*(7), 1075–1087.
- Smith, S. M., Jenkinson, M., Woolrich, M. W., Beckmann, C. F., Behrens, T. E., Johansen-Berg, H., et al. (2004). Advances in functional and structural MR image analysis and implementation as FSL. *NeuroImage*, *23*, 208–219.
- Sowell, E. R., Thompson, P. M., & Toga, A. W. (2004). Mapping changes in the human cortex throughout the span of life. *Neuroscientist*, *10*(4), 372–392.
- Sullivan, E. V., Rosenbloom, M., Serventi, K. L., & Pfefferbaum, A. (2004). Effects of age and sex on volumes of the thalamus, pons, and cortex. *Neurobiology of Aging*, *25*(2), 185–192.
- Taki, Y., Goto, R., Evans, A., Zijdenbos, A., Neelin, P., Lerch, J., et al. (2004). Voxel-based morphometry of human brain with age and cerebrovascular risk factors. *Neurobiology of Aging*, *25*(4), 455–463.
- Talairach, J., & Tournoux, P. (1988). *Co-planar stereotaxic atlas of the human brain: 3-Dimensional proportional system—An approach to cerebral imaging*. New York: Theme Medical Publishers.
- Tang, Y., Hojatkashani, C., Dinov, I. D., Sun, B., Fan, L., Lin, X., et al. (2010). The construction of a Chinese MRI brain atlas: A morphometric comparison study between Chinese and Caucasian cohorts. *NeuroImage*, *51*, 33–41.
- Thompson, P. M., Mega, M. S., Woods, R. P., Zoumalan, C. I., Lindshield, C. J., Blanton, R. E., et al. (2001). Cortical change in Alzheimer's disease detected with a disease-specific population-based brain atlas. *Cerebral Cortex*, *11*(1), 1–16.
- Thorpe, S. G., Cannon, E. N., & Fox, N. A. (2014). Spectral and source structural development of mu and alpha rhythms from infancy through adulthood. Unpublished manuscript.
- Toga, A. W., Thompson, P. M., & Sowell, E. R. (2006). Mapping brain maturation. *FOCUS: The Journal of Lifelong Learning in Psychiatry*, *4*(3), 378–390.
- Tsuzuki, D., Cai, D. S., Dan, H., Kyutoku, Y., Fujita, A., Watanabe, E., et al. (2012). Stable and convenient spatial registration of stand-alone NIRS data through anchor-based probabilistic registration. *Neuroscience Research*, *72*(2), 163–171.
- Tsuzuki, D., Jurcak, V., Singh, A. K., Okamoto, M., Watanabe, E., & Dan, I. (2007). Virtual spatial registration of stand-alone fNIRS data to MNI space. *NeuroImage*, *34*(4), 1506–1518.
- Tzourio-Mazoyer, N., Landeau, B., Papathanassiou, D., Crivello, F., Etard, O., Delcroix, N., et al. (2002). Automated anatomical labeling of activations in SPM using a macroscopic anatomical parcellation of the MNI MRI single-subject brain. *NeuroImage*, *15*(1), 273–289.
- Vanderwert, R. E., & Nelson, C. A. (2014). The use of near-infrared spectroscopy in the study of typical and atypical development. *NeuroImage*, *85*, 264–271.
- Waber, D. P., De Moor, C., Forbes, P. W., Almlí, C. R., Botteron, K. N., Leonard, G., et al. (2007). The NIH MRI study of normal brain development: Performance of a population based sample of healthy children aged 6 to 18 years on a neuropsychological battery. *Journal of International Neuropsychological Society*, *13*(5), 729–746.
- Weisenfeld, N. I., & Warfield, S. K. (2009). Automatic segmentation of newborn brain MRI. *NeuroImage*, *47*(2), 564–572.
- Wilke, M., Holland, S. K., Altaye, M., & Caser, C. (2008). Template-O-Matic: A toolbox for creating customized pediatric templates. *NeuroImage*, *41*(3), 903–913.

- Wilke, M., Schmithorst, V. J., & Holland, S. K. (2002). Assessment of spatial normalization of whole-brain magnetic resonance images in children. *Human Brain Mapping, 17*(1), 48–60.
- Woolrich, M. W., Jbabdi, S., Patenaude, B., Chappell, M., Makni, S., Behrens, T., et al. (2009). Bayesian analysis of neuroimaging data in FSL. *NeuroImage, 45*(1), S173–S186. <http://dx.doi.org/10.1016/j.neuroimage.2008.10.055>.
- Xie, W., Richards, J. E., Lei, D., Kang, L., & Gong, Q. (2014a). Comparison of the brain development trajectory between Chinese and U.S. children and adolescents. Submitted.
- Xie, W., Richards, J. E., Lei, D., Kang, L., & Gong, Q. (2014b). The construction of MRI brain/head templates for Chinese children from 7–16 years of age. Submitted.
- Xue, H., Srinivasan, L., Jiang, S., Rutherford, M., Edwards, A. D., Rueckert, D., et al. (2007). Automatic segmentation and reconstruction of the cortex from neonatal MRI. *NeuroImage, 38*(3), 461–477.
- Yakovlev, P. I., & Lecours, A. R. (1967). The myelogenetic cycles of regional maturation of the brain. In A. Minkowski (Ed.), *Regional development of the brain in early life* (pp. 3–70). Oxford: Blackwell Science.
- Yoon, U., Fonov, V. S., Perusse, D., & Evans, A. C. (2009). The effect of template choice on morphometric analysis of pediatric brain data. *NeuroImage, 45*(3), 769–777.
- Zhang, Y. Y., Brady, M., & Smith, S. (2001). Segmentation of brain MR images through a hidden Markov random field model and the expectation maximization algorithm. *IEEE Transactions on Medical Imaging, 20*(1), 45–57.
- Zieber, N., & Richards, J. E. (2013). *Developmental changes in the infant N290 in response to faces and toys*. Poster presented at the Society for Research in Child Development, Seattle, WA, April 2013.